Wu, Jin; Chavana-Bryant, Cecilia; Prohaska , Neill; Serbin, Shawn P.; Guan, Kaiyu; Albert, Loren P.; Yang, Xi; van Leeuwen, Willem J.D.; Garnello, Anthony John; Martins, Giordane; Malhi, Yadvinder; Gerard, France; Oliviera, Raimundo Cosme; Saleska, Scott R. 2017. **Convergence in relationships between leaf traits, spectra and age across diverse canopy environments and two contrasting tropical forests** [in special issue: Featured papers on 'Tropical plants and ecosystem function'] *New Phytologist*, 214 (3). 1033-1048. 10.1111/nph.14051

Convergence in relations among leaf traits, spectra and age across diverse canopy environments and two contrasting tropical forests

Authors

Jin Wu[1*], Cecilia Chavana-Bryant[2], Neill Prohaska[1], Shawn P. Serbin[3], Kaiyu Guan[4], Loren P. Albert[1], Xi Yang[5], Willem J.D. van Leeuwen[6], Anthony John Garnello[1], Giordane Martins[7], Yadvinder Malhi[2], France Gerard[8], Raimundo Cosme Oliviera[9], and Scott R. Saleska[1*]

Institute or laboratory of origin

[1] Department of Ecology and Evolutionary Biology, University of Arizona, Tucson, AZ 85721

[2] Environmental Change Institute, School of Geography and the Environment, University of Oxford, UK

[3] Biological, Environmental & Climate Sciences Department, Brookhaven National Lab, Upton, New York, NY 11973

[4] Department of Natural Resources and Environmental Sciences, University of Illinois at Urbana Champaign, Urbana, IL 61801

[5] Department of Earth, Environmental, and Planetary Sciences, Brown University, Providence, RI 02912

[6] School of Natural Resources and the Environment, University of Arizona, Tucson, AZ 85721

[7] Brazil's National Institute for Amazon Research (INPA), Manaus, Amazonas, Brazil

[8] Centre for Ecology and Hydrology (CEH), Wallingford, Oxfordshire OX10 8BB, UK

[9] Embrapa Amazônia Oriental, Pará, Brazil

***Corresponding author**

Tel. +1 (520) 704-5358; Fax +1 (520) 621-9190; jinwu@email.arizona.edu (J.W.), saleska@email.arizona.edu (S.R.S)

Keywords: Spectroscopy, partial least squares regression (PLSR), vertical canopy profiles, leaf mass per area (LMA), leaf water content (LWC), vegetation indices, understory

Type of Paper: Original Research

Word Count:

Summary: 201 words

Main-Text--

Introduction: 1002 words

Methods: 2352 words

Results: 1681 words

Discussion/Conclusion: 1614+375 words

Acknowledgement: 118 words

9 Figures 1 Table

Supplementary materials: 7 Figures 2 Table

A submission for the Special Issue "*Plant traits and ecosystem function along tropical environmental gradients: from leaves to landscapes*"

Summary

- Leaf age structures the phenology and development of plants, as well as the evolution of leaf traits over life histories. However, a general method for efficiently estimating leaf age across forests and canopy environments is lacking.
- We explored the potential for a statistical model, previously developed for Peruvian sunlit leaves, to consistently predict leaf ages from leaf reflectance spectra across two contrasting forests in Peru and Brazil and across diverse canopy environments.
- The model performed well for independent Brazilian sunlit and shade canopy leaves (R^2=0.75-0.78), suggesting that canopy leaves (and their associated spectra) follow constrained developmental trajectories even in contrasting forests. The model did not perform as well for middle-canopy and understory leaves (R^2=0.27-0.29), because leaves in different environments have distinct traits and trait developmental trajectories. When we accounted for distinct environment-trait linkages—either by explicitly including traits and environments in the model, or, even better, by re-parameterizing the spectra-only model to implicitly capture distinct trait-trajectories in different environments—we achieved a more general model that well-predicted leaf age across forests and environments (R^2=0.79).
- Fundamental rules, linked to leaf environments, constrain development of leaf traits and allow for general prediction of leaf age from spectra across species, sites and canopy environments.

1. Introduction:

It has long been recognized that many important ecological processes vary with leaf age, the time elapsed since leaf budburst. During their lifetime, leaves exhibit variable photosynthetic rates (Field, 1983; Reich *et al*., 1991; Wilson *et al*., 2001; Kitajima *et al*., 2002; Pantin *et al*., 2012), morphological changes (Maksymowych, 1973), allocation and transformation of chemicals (Wilson *et al*., 2001; Kitajima *et al*., 2002; Pantin *et al*., 2012), epiphyll colonization (Roberts *et al*., 1998; Toomey *et al*., 2009), and defense against herbivory (Coley, 1980; Coley & Barone, 1996; Lawrence *et al*., 2003; Wang *et al*., 2012). Thus, leaf age is a critical parameter for interpreting leaf function over time and for understanding how leaf traits evolve over

development. Furthermore, expected maximum leaf age (leaf lifespan) is central to understanding plant life history (Field & Mooney, 1983; Reich *et al.*, 1992), population dynamics (Reich *et al.*, 2004) and the evolutionary trade-offs of the leaf economic spectrum (Reich *et al.*, 1997; Wright *et al.*, 2004; Funk & Cornwell, 2013; Osnas *et al.*, 2013). Thus, many disciplines have long been interested in monitoring leaf age for individual plants (Field, 1983; Roberts *et al.*, 1998; Wilson *et al.*, 2001; Reich *et al.*, 2004) and leaf lifespan for many species (Reich *et al.*, 1991, 1992; Wright *et al.*, 2004; Funk & Cornwell, 2013; Osnas *et al.*, 2013).

More recent studies have begun to emphasize the importance of leaf ages and canopy age composition on phenology and ecosystem seasonality of vegetation photosynthesis and transpiration (Doughty & Goulden, 2008; Richardson *et al.*, 2012; Restrepo-Coupe *et al.*, 2013; Wu *et al.*, 2016). Yet leaf development is difficult to monitor at large scales, especially in carbon rich tropical evergreen forests, where individual leaf ages are not as tightly synchronized with phenology and ecosystem seasonality as in temperate forests (Reich, 1995). In tropical forests, contrasting interpretation of satellite-detected seasonality of vegetation greenness (Morton *et al.*, 2014; Bi *et al.*, 2015; Saleska *et al.*, 2016) arises, in part, due to differing assumptions about the distribution of leaf ages in forest canopies and how changes in age composition might affect ecosystem seasonality (Doughty & Goulden, 2008; Brando *et al.*, 2010; Morton *et al.*, 2014). Therefore, for such forests, 'ground truth' studies of seasonal leaf age dynamics are clearly needed.

Despite the broad interest in leaf aging, there is currently no efficient and rapid method for estimating leaf age that can be applied across forests. Previous studies linking leaf morphological development (e.g. leaf length) to leaf aging (Erickson & Michelini, 1957; Chen *et al.*, 2009; Meicenheimer, 2014) involved laborious measurements over long time periods or relied on uncertain assumptions. Near-surface remote sensing, e.g. via "phenocam", is an alternate technique for approximating leaf age of canopy trees in temperate deciduous forests (Richardson *et al.*, 2009; Keenan *et al.*, 2014). This approach, however, has not been tested in tropical evergreen forests and its application could prove challenging due to the high diversity of leaf phenologies, with many tree species being brevi-deciduous or evergreen during most or all of the annual cycle (Opler *et al.*, 1980; Reich, 1995; Schöngart *et al.*, 2002).

Spectroscopy may provide a fast and efficient means for estimating leaf ages from their optical properties. Differences in the reflectance, absorbance, and transmittance of light at

different wavelengths by plant parts are tightly coupled to their chemical composition, cell structure, and physiological properties (Curran, 1989; Elvidge, 1990; Kokaly *et al*., 2009), leading to the rapid recent development of spectroscopic methods as a general tool in plant ecophysiology and ecology. For example, spectroscopy has been used to estimate wood density and hydraulic traits (Acuna & Murphy, 2006; Petisco *et al.*, 2006; Luss *et al*., 2015), accurately identify plant species from dried leaves (Durgante *et al*., 2013) across developmental stages (Lang *et al*., 2015), quantify non-structural carbohydrate content of different plant organs (Ramirez *et al*., 2015), and characterize a broad suite of leaf biophysical traits (Clark *et al.*, 2005; Asner & Martin, 2011; Asner *et al*., 2014; Serbin *et al*., 2012, 2014).

Chavana-Bryant *et al* (2016), also in this special issue, was the first study to demonstrate that leaf reflectance spectra can successfully predict leaf age by using a partial least squares regression (PLSR, Wold *et al.*, 2001) approach applied to data from a Peruvian evergreen forest. The underlying logic motivating the development of this spectra-age model was that because (1) leaf traits follow consistent developmental trajectories as leaves age, (2) leaf spectra emerge from the ensemble of traits that define a leaf's structure and function at any particular time (Asner *et al*., 2014; Serbin *et al*., 2012, 2014; Ramirez *et al*., 2015), leaf spectra may be directly used to estimate leaf ages, and indeed, be a better predictor of leaf age than any particular limited set of leaf traits.

Although the spectra-age model was successfully tested for sunlit leaves in an evergreen forest in Peru (Chavana-Bryant *et al*., 2016), the broader applicability and potential limitations of this approach were not explored. This study thus focuses on exploring factors that might limit the model performance, such as variation in age-trait or age-spectra relations across forest sites and diverse canopy environments, where species composition, leaf types and trait values all vary. Specifically, we aim to answer the following questions:

1. How are leaf traits and spectra related with leaf development across sites and canopy environments?
2. Are these relationships sufficiently consistent to allow a general model to accurately predict leaf age from spectra across sites and various canopy environments?

To address these questions, we used measurements of reflectance spectra, traits, and age of leaves collected at two tropical evergreen forests: we built upon the spectra-age model presented in Chavana-Bryant *et al* (2016) that was based on sunlit leaves of a Peruvian Amazonian forest

and evaluated this model at an independent Brazilian site with contrasting soil and forest properties. We then explored the consistency of relationships across both sites, with a view to developing and validating a spectra-age model generally applicable for tropical forest leaves across forest sites and canopy environments.

2. Materials and Methods

2.1 Study Sites

The study focuses on two Amazonian evergreen forests (Fig. 1): a Brazilian site and a Peruvian site that represent contrasting edaphic and forest properties along the primary axis of ecological variation across Amazonian forests. The Brazil site is less productive, higher wood density and slower turnover but higher biomass forest than the Peru site (Malhi *et al.,* 2002, 2006; *Patino et al.*, 2009). The contrast appears driven by soil properties, with western Amazonian soils in Peru being more fertile but with poorer physical structure (Quesada *et al.*, 2012).

The Brazil site (2°51' S, 54°58' W) encompasses the km67 eddy flux tower and associated biometric plots in Tapajos National forest, near Santarém, Brazil (Rice *et al.,* 2004; Hutyra *et al*., 2007). Part of the Brazilian Large Scale Biosphere-Atmosphere Experiment in Amazonia (LBA) (Davidson *et al*., 2012), this site sits on a well-drained clay-soil plateau. Mean annual precipitation is ~2000 mm/year with a 5-month-long dry season (Restrepo-Coupe *et al*., 2013).

The Peru site encompasses two primary forest plots within the Tambopata National Reserve in the Madre de Dios region of Peru (Malhi *et al*., 2014), both part of the Global Ecosystems Monitoring (GEM) network and the RAINFOR Amazon Forest Inventory Network (Malhi *et al.*, 2002), with RAINFOR codes TAM-06 (12°84' S, 69°30' W) and TAM-09 (12°83' S, 69°27' W). These forests grow on Haplic alisol soils (Quesada *et al.*, 2010), at elevations of 215m and 220m above sea level, respectively. Mean annual precipitation is ~1900 mm/year (Malhi *et al.*, 2014), with a 4-5 month-long dry season (precipitation <100 mm/mo; Lewis *et al.*, 2011).

2.2 Field measurements

2.2.1 Brazil dataset

In campaigns conducted in August-September 2013, November 2013, March 2014, and July-August 2014, we selected a subset of 11 trees (Table 1) for precise leaf age monitoring. The age monitoring began with observations of leaf budburst and subsequent leaf tagging (using metal

tags alongside *in-situ* photos; Fig. S1) during the August-September 2013 campaign, when most sampled trees were flushing new leaves. Following the initial intensive tagging work, we continued to tag and photograph new leaves periodically. This age tagging technique enabled us to accurately track leaf age in terms of days from leaf emergence at budburst (0 days) to old age (~400 days). Aside from some of the canopy leaves, this age was not sufficient to sample the senescent leaf age class.

We sampled a total of 759 leaves with precise leaf age information for these 11 trees, consisting of 4 canopy, 3 mid-canopy, and 4 understory trees. Since we harvested both sunlit and shaded leaves for canopy trees, our dataset of precise leaf age measurements is composed of 15 tree-environment combinations: leaves sampled from 4 canopy trees in a sunlit environment, 4 canopy trees in a shaded environment, 3 mid-canopy trees environment, and 4 understory trees environment (Table 1).

We measured reflectance spectra (section 2.2.3) for all 759 leaves and leaf traits (Leaf Mass per Area, LM, and Leaf Water Content, LWC) for a subset of 507 of these leaves which were used for the trait-age analysis reported here. Traits were derived from fresh leaf weight (precision at 0.001 g), area (using a Canon LiDE 120 scanner) and dry weight oven-dried at 60 ^{o}C for 72 hours.

We recorded leaf growth environments, including (1) *in-situ* digital hemispherical photos (collected with a 180° fisheye lens adapter for a Canon T3) to capture the radiation regime (section 2.2.5), (2) branch height (m)—the height of sampled leaves aboveground, and (3) branch depth (m)—the depth of sampled leaves below local canopy top.

In addition to the 11 trees with precisely measured leaf ages, we sampled an additional 29 tree species across diverse canopy environments, including 7 canopy trees (crowns exposed to direct sun), 10 mid-canopy trees (20-30m tall), 4 understory trees (10-20m tall), and 8 forest-floor shrubs (<5 meters tall). The dataset included measurements of leaf traits (LMA and LWC), reflectance spectra, and the canopy environments (i.e. vertical canopy positions where the leaves were harvested). This dataset did not include precise leaf ages, but provides baseline data on community level relationships between leaf traits and canopy environments for fully expanded mature leaves (Fig. S4).

2.2.2 Peru dataset

The Peru dataset of 1072 leaves was collected in 2011, for sunlit leaves of 12 canopy trees (see Table 1 for species list). Measurements encompassed two leaf functional traits (LMA, and LWC), and associated leaf reflectance spectra. Peru leaves were assigned a leaf age designed to correspond to their developmental stage, with young leaves first assigned an initial age of 1 week when they reached a size large enough to be measured for spectra, and thereafter tracked through time until they reached advanced senescence (~400 days). Old leaves (> ~250 days) had their ages adjusted by normalization relative to maximum leaf age at senescence, taken to be 13 months (see Chavana-Bryant *et al.*, 2016; Fig. 1). Full details of the data collection and leaf age classification protocols for this site are reported in Chavana-Bryant *et al* (2016).

We note that this method of assigning leaf ages differed from that used in Brazil, where absolute ages (based on time elapsed since tagging at emergence) were used for all leaves. This difference in age assignment methods results in a 1-4 week offset in age between the datasets, depending on species (Brazil tagged leaves were measured for spectra when they were sufficiently large, typically at 2-5 weeks since emergence, an age that was defined as 1 week for Peru leaves), and a scale difference, depending on species, for old leaves (since Peru leaves were scaled to reach senescence at 13 months whereas Brazil leaf ages were tracked to about 13 months without scaling). As shown in the results section, this difference in dating methods did not significantly limit the inter-comparability of leaf age predictions between sites.

2.2.3 Spectral measurements in Brazil

We measured leaf spectra using a full-range (350-2500nm) FieldSpec® Pro spectroradiometer (Analytical Spectra Devices, ASD, Boulder, CO). The spectrometer had a spectral sampling resolution of 1.4nm, 2.2nm and 2.3nm in the visible, NIR, and SWIR wavelengths and all data were interpolated to 1nm before analysis. All measurements were collected using a customized assembly attached to a plant probe with an internal calibrated light source, following Chavana-Bryant *et al* (2016) protocols. The customized assembly was composited by two measurement blocks: one for 99.9% reflectivity white standard (Spectralon, Labsphere Inc., North Dutton, NH, USA), and the other for 3% reflectivity dark standard (Odyssey III black 449/9009 Marine Grade Cover Fabric). For each leaf, reflectance spectra were measured on 1-6 different parts of the leaf adaxial surface and then averaged to determine the mean optical properties across all wavelengths.

233

234 2.2.4 Vegetation indices (VIs)

235 To include important aspects of leaf bio-physiological traits that are not fully covered by
236 LMA and LWC, we calculated four commonly-used VIs, including Normalized Difference
237 Vegetation Index (NDVI; Eqn 1; Tucker, 1979; Ustin *et al*., 2009), Enhanced Vegetation Index 2
238 (EVI2; Eqn 2; Jiang *et al*., 2008), Photosynthetic Reflectance Index (PRI; Eqn 3; Gamon *et al*.,
239 1992), and Normalized Difference Water Index (NDWI; Eqn 4; Gao, 1996).

240
$$NDVI = \frac{NIR - R}{NIR + R} \quad (1)$$

241
$$EVI2 = 2.5 \times \frac{NIR - R}{NIR + 2.4 \times R + 1} \quad (2)$$

242
$$PRI = \frac{\rho_{531} - \rho_{570}}{\rho_{531} + \rho_{570}} \quad (3)$$

243
$$NDWI = \frac{NIR - SWIR}{NIR - SWIR} \quad (4)$$

244 where NIR is the reflectance at near-infrared 800 nm band, R is the reflectance at Red 680 nm
245 band, ρ_{531} is the reflectance at 531 nm, ρ_{570} is the reflectance at 570 nm, and SWIR is the
246 reflectance at short-wavelength infrared 1240 nm band.

247 These VIs represent important leaf bio-physiological properties: NDVI and EVI2 are the
248 integrated metric for the greenness and structure of leaves (Sellers *et al.,* 1992; Huete *et al.*,
249 2002); PRI is a measure of the intrinsic quantum yield for photosynthesis (Gamon *et al.*, 1992);
250 NDWI is an indicator of leaf water content or hydrological status (Gao, 1996). By using these
251 VIs (together with leaf traits of LMA and LWC, and spectra), we aim for a more comprehensive
252 understanding of canopy environments effect on leaf properties and their developmental
253 trajectories.

254

255 2.2.5 Within-canopy light environment

256 We estimated the within-canopy light environment from *in-situ* digital hemispheric photos
257 (section 2.2.2). These photos were preprocessed and quality controlled using Adobe Lightroom 4
258 (Adobe Systems INC., San Jose, CA). Contrast was then optimized, and the modified images
259 were exported in JPEG format. Using a custom MATLAB program together with Otsu's

algorithm (Ostu, 1975), these images were automatically binarized into sky (or gap) or non-sky pixels. The image fraction of the sky, or gap fraction, was then calculated to index the light environment of the leaf sample.

2.3 Spectra-Age Modelling

2.3.1 General approach

As in Chavana-Bryant *et al* (2016), we used the partial least-square regression (PLSR) modeling approach (Geladi & Kowalski, 1986; Wold *et al*., 2001), which was adapted from several recent studies (Wolter *et al*., 2008; Serbin *et al*., 2014; Singh *et al*., 2015). PLSR is the current state-of-the-art approach for linking leaf and canopy spectroscopy with leaf and plant traits (e.g. Bolster *et al.*, 1996; Townsend *et al.*, 2003; Asner and Martin, 2011; Serbin *et al.*, 2014). Previous studies have also shown that PLSR is a more robust method compared to simple correlation or multiple linear regression approaches (Geladi & Kowalski, 1986; Grossman et al., 1996; Wold *et al*., 2001).

Here the PLSR included five steps (Fig. S2): (1) filtering of outliers (which removed ~5% of data) following the Monte-Carlo sampling method for outlier detection (Xu & Liang, 2001); (2) the filtered dataset was one-time randomly divided into the training (70%) and testing (30%) datasets; (3) 90% of the training dataset were randomly selected (with 100-time replication) for PLSR analysis, with the latent variable number varying from 1 to n (n=20 in our case); (4) the PLSR regression coefficients were applied to the training and testing datasets, with model performance assed by using root mean squares error (RMSE), and R^2 (the proportion of variance of observation explained by model); (5) the optimal latent variable number were then identified by minimizing RMSE and maximizing R^2.

We implemented the above PLSR analysis to our predictor variables, using the MCS function from LibPLS (http://www.libpls.net) for outlier removal, PLSREGRESS function in Matlab (Mathworks, Natick, MA, USA) for the PLSR analysis, and custom Matlab functions for other steps. The predictor variables in this study can be either leaf spectra only (400–2500 nm; see "Peru Spectra model" in section 2.3.2 and "All Spectra model" in section 2.3.3 below) or leaf spectra combined with leaf traits (see "Peru Spectra+all Trait model" and "All Spectra+all Trait model" in section 2.3.3 below).

291 2.3.2 Cross-site spectra-age analysis

292 We first examined the ability to model leaf age from leaf spectra across different sites
293 through a series of tests. We used the spectra-age model developed for Peruvian sunlit leaves
294 (Chavana-Bryant *et al.*, 2016) as a "reference model" (or "original Peru Spectra model"),
295 applying it to the Brazilian dataset which included leaves sampled from four canopy
296 environments. The goal was to explore the potential for generalizing the spectra-age model
297 across sites (from Peruvian sunlit leaves to Brazilian sunlit leaves) and across canopy
298 environments (from Peruvian sunlit leaves to Brazilian canopy shade, middle-canopy and
299 understory leaves).

300

301 2.3.3 Generalizing the leaf age model across canopy environments

302 Since leaf growth environments affect within-canopy leaf trait variation (Ellsworth & Reich,
303 1993; Cavaleri *et al*., 2010), we expected that the leaves from the broader range of growth
304 environments in Brazil would have different optical properties (and therefore different
305 relationships between leaf spectra and age) as compared with the sunlit leaves from Peru
306 (Chavanna-Bryant *et al.,* 2016). To investigate how spectra-age relationships depend on the
307 different growth environments and their associated traits, and hence, to develop a more general
308 model of leaf age applicable across these growth environments, we first conducted a reference
309 test ("Test 0") of how well the original Peru Spectra model predicted leaves across different sites
310 and environments. We then tested three models of leaf age--trait--spectra relations across canopy
311 environments:

312 - Test 1 (Peru Spectra+ all Trait model) —determines whether accounting for changing
313 growth environments and their associated leaf traits could improve performance of the
314 Peru reference model when applied to leaves from all environments. To this end, we used
315 the original leaf spectral variables for the Peru reference model alongside the added
316 variables, including branch height, depth, LMA, LWC, and four VIs, as the new predictor
317 variables, to generate a "Peru Spectra+all Trait" PLSR model.
318 - Test 2 (All Spectra model) —tests whether a more general spectra-only model can predict
319 leaf ages across all categories of leaves and growth environments. In this test, we used
320 combined Peru and Brazil datasets (with leaves encompassing the full range of traits that

emerge from development under different environments) to re-parameterize an "All Spectra" model (with no traits included explicitly).

- Test 3 (All Spectra+all Trait model) is a simple combination of test 1 and 2.

We hypothesized (**H1**) that including traits and proxies for growth environments (test 1) would indeed improve model generality from sunlit leaves to understory leaves. A positive outcome for test 1 (which would show that accounting for environmental influence on leaf trait variation improves ability to predict age) would suggest a second hypothesis (**H2**) that a spectra-only model should be able to perform as well as, or even better than, the hybrid model of Test 1. This is because spectral models have been shown to predict a broad array of traits (e.g. Serbin *et al.*, 2014), including traits that are unmeasured for the leaves used in this study but which may also be associated with age (Chavana-Bryant *et al.*, 2016). Finally, we hypothesize (**H3**) that test 3 will perform only marginally better than test 2, because the spectra will themselves already capture the majority of the variation in the response as compared to including traits separately in the model.

To test these hypotheses, in addition to the two metrics of model goodness, RMSE and R^2 (section 2.3.1 above), we also calculated the Akaike Information Criterion (AIC) for the model cross-comparisons. The AIC used is formatted as $AIC = N \times \log(\delta^2) + 2 \times m$, following the literature (Akaike, 1974; Aho *et al.,* 2014), where N is the number of leaves, δ is RMSE, and m is the optimal latent variable number for each PLSR modeling scenario (section 2.3.1 above).

3. Results

We first focus on the results from the Brazil site (reported here for the first time), and then show integration with the Peru dataset (from Chavanna-Bryant *et al.*, 2016).

3.1 Leaf traits and spectra vary with age across canopy environments and forests

Despite the broad trait variation induced by different canopy environments (from full sun to deeply shaded understory environment, Table S1), correlations of leaf traits LMA and LWC with leaf age were evident across the Brazilian site community (R^2=0.20, $p<10^{-5}$ for LMA; R^2=0.42, $p<10^{-5}$ for LWC; Fig. 2a,b). The trait differences across canopy environments tended to obscure the strength of these correlations, which were more evident within specific environments across all trees (R^2=0.23 to 0.72 for LMA and R^2=0.60 to 0.80 for LWC, Fig. 2) and within

environments of individual trees. Within individual trees, all 11 tree-environment combinations showed a significantly positive trend in LMA-age relationships (R^2=0.52-0.91), and significantly negative LWC-age relationships (R^2=0.60-0.95). These positive LMA-age and negative LWC-age relationships are consistent with those that were observed at the contrasting forest in Peru where a single leaf environment was sampled (sunlit leaves, Chavana-Bryant *et al.*, 2006).

Spectral data also showed strong dependency on leaf age and leaf canopy environment across all Brazilian tree-environment combinations (Fig. 3 and Fig. S7). Mean visible reflectance, especially the green peak (~550 nm), and its variance showed continuous declines with age across all Brazilian tree-environment combinations. Initial mean NIR reflectance (800-1200 nm) increased (with lower variance) during leaf expansion, which was followed by decreases in the mean (and increases in variance) as leaves aged (Fig. 3a,c). Mean SWIR reflectance (1400-2500 nm) increased monotonically with age, while the variance initially decreased and then increased as leaves aged. These patterns of the relative spectra change with leaf age, observed at the Brazil site across vertical canopy profiles, are also consistent with those observed in the Peruvian sunlit leaves (Chavana-Bryant *et al.*, 2016).

Strong spectral dependencies on canopy environments were also observed (Fig. 3b). Upper canopy versus middle canopy or understory differences were especially strong in the SWIR, where reflectance increased monotonically with depth into the canopy (Fig. 3d). Effects due to canopy growth environment were comparable to those of leaf age, indicating that models intended to predict age across different canopy environments would likely need to account for growth environment effects.

3.2 Cross-site spectra-age analysis

Since leaf traits and spectra consistently vary with leaf age across both canopy environments and forest sites (albeit with offsets among the different canopy environments), we explored the application of the Peru-trained spectra-age model to the independent forest in Brazil. We found that the Peruvian model developed in Chavana-Bryant *et al* (2016, with 7 latent variables) predicted ages of leaves for the Brazilian canopy trees with high precision (R^2=0.75 and R^2=0.78 for sunlit and shade canopy leaves respectively) (see Fig 4a,b at 7 latent variables, and Fig. 9a). However, model performance when predicting ages of leaves from middle and understory

Brazilian trees was poor (R^2=0.27 and R^2=0.29 for Brazilian middle-canopy and understory leaves respectively) (Fig 4a,b for 7 latent variables; Fig. 9a).

We sequentially re-fitted the Peru-trained model with different numbers of latent variables, in order to investigate whether there existed an optimum number of latent variables that would improve the Peru-trained model performance across the range of canopy environments at the Brazil site. We found that reducing the number of latent variables from 7 to 5 significantly improved performance of the Peru-trained model in predicting the ages of Brazil middle-canopy and understory leaves, without resulting in a significant reduction in performance for Peruvian sunlit leaves (for which the 7-variable model was optimal) (Fig. 4a,b). We thus adopted the 5-variable model as the Peru reference model, optimized across canopy environments.

Closer investigation of the performance of the 7-variable Peru-trained spectra-age model for individual Brazilian trees revealed that the relatively poor performance of this model relative to the 5-variable model was confined to early developing leaves (≤40 days old) of one middle-canopy and two understory trees (*E.uchi*_MC, *G.Amazonicum*_US, and *M.ruficalyx*_US; Table 1 and Fig. 5). The early developing leaves of these trees exhibited "reddish" coloration (e.g. Fig. 5a), a common early developmental process displayed by sub-canopy leaves but not by canopy sunlit leaves, which has confounding effects for the 7-variable Peru model (Fig. 5c).

The PLSR regression coefficients (Fig. 4c) and Variable Importance in Projection (VIP; Fig. 4d) from this optimized reference model indicated the important spectral domains responsible for leaf age modeling, which included visible domain (especially ~550 nm), red edge (~725 nm), NIR (~800 nm) and several water absorption bands (~1440 nm, ~1700 nm, and ~1920 nm). These patterns also matched well with the age-dependent spectral variation (Fig. 3a,c), providing confidence for our spectra-age modeling.

The optimized Peru model performance using the Peru testing data was R^2=0.83 and RMSE=55 days compared with R^2=0.64 and RMSE=72 days when applied to all Brazilian data (Fig. 9b). When the Brazil data were separated by canopy environments, cross-site performance of the Peru model applied to the Brazil data ranged from high performance in sunlit and shade canopy leaves and middle-canopy leaves (R^2=0.77, RMSE=62 days for sunlit, and R^2=0.77, RMSE=62 days for shade canopy leaves, and R^2=0.71, RMSE=80 days for middle-canopy leaves) to lower performance when applied to understory leaves (R^2=0.29, RMSE=101 days for the original Peru model and R^2=0.47, RMSE=90 days for the optimized Peru model) (Fig. 9a,b). In

sum, we found that the greater the disparity in canopy environment from that used to train the Peru reference model, the larger the inaccuracies in leaf age model predictions.

3.3 The range of leaf traits affects cross-site model generality

We investigated whether the relatively lower performance of the Peru-trained canopy sunlit leaf age model for leaves sampled from canopy environments beyond its original scope was associated with different suites of traits and/or developmental pathways not included in the reference model training dataset, and if so, whether such differences were systematically linked to the broader range of canopy environments. We found that canopy sunlit leaves from the two sites largely overlapped in both their height above the ground (a proxy for growth environment), and in their trait values, but that sunlit leaves were significantly different from understory leaves in growth-environments and leaf trait values for old leaves (Fig. 6). The presence of 'reddish' early developmental leaves in the middle canopy and understory also demonstrates the existence of a different developmental pathway. This environmentally driven divergence in traits (as also seen in Ellsworth & Reich, 1993; Cavaleri *et al*., 2010) provides a mechanistic basis for improving predictive models of leaf age applicable across canopy growth environments.

To leverage this result, we quantified how model fit of the optimized Peru reference model (developed for Peruvian sunlit leaves) depended on different environments. Deviations of predictions from observations were characterized by simple linear regressions for each tree-environment combination (as seen by regression lines between model predicted and observed ages, Fig. 7). These regression lines showed systematic deviation from the 1:1 line, with strong dependency on leaf growth environments: Deviations in canopy sunlit environments (Fig. 7a-d) usually (3 of 4 trees) followed a slope shallower than the 1:1 line, while at the other end of the environmental gradient, deviations in Brazilian understory trees were significantly steeper than the 1:1 line (Fig. 7l-o). Deviations were largest in understory environments, whose leaf ages tended to be significantly overestimated in young age classes, but underestimated in old age classes.

We found that the deviation of leaf age model performance could be tied to canopy environments (and to leaf traits): the deviations, as represented by the variation in the parameters (slope and intercept) of lines fit to those deviations, were systematically explained by growth environments, as captured by branch height (Fig. 8a,c), and by traits (e.g. LMA, Fig. 8b,d).

Therefore, variability in canopy environments and traits is the source of the lower performance of the optimized Peru leaf age model when extended to new canopy environments. This suggests that modeling strategies that account for variation in traits or proxies for canopy environment (e.g. branch height) should produce more general models of leaf age that are applicable across different canopy growth environments.

3.4 Generalizing the leaf age model across canopy environments

Four modeling exercises were conducted to explore model generality across canopy environments in Brazil (Fig. 9), with the optimum five latent variables for "Peru Spectra" and "All Spectra" models and the optimum six latent variables for "Peru Spectra+all Trait" and "All Spectra+all Trait" models (Fig. S6). The calculated AIC metric for each modeling scenario showed consistent, positive relationship with RMSE, suggesting that RMSE is a good metric for the cross-model comparison in this study (Table S2). Relative to the Peru reference model (Fig. 9a), the "Peru Spectra+all Trait" model, which incorporated the covariates of growth environments and leaf traits, modestly improved overall performance for all the Brazil data (R^2=0.69, RMSE=74 days *vs* R^2=0.64, RMSE=72 days for reference; Fig. 9c), but significantly improved prediction for Brazilian understory samples (R^2 increased from 0.47 to 0.57; RMSE decreased from 90 days to 88 days).

The "All Spectra" model, parameterized by both Peruvian and Brazilian leaf spectra (Fig. 9d), achieved large performance gains across canopy environments (R^2 increased from 0.64 to 0.79 and RMSE decreased from 72 days to 53 days for all Brazilian leaves; R^2 increased from 0.47 to 0.73 and RMSE decreased from 90 days to 72 days for Brazilian understory leaves).

The "All Spectra+all Trait" model, parameterized by both Peruvian and Brazilian leaf spectra and traits (Fig. 9e), led to the best model overall, but, as we hypothesized (H3 from §2.3.3 above), it gave only a modest improvement over the "All Spectra" model overall (R^2 increased from 0.79 to 0.81 and RMSE decreased from 53 days to 50 days; Fig. 9). Specifically, the most significant improvement occurred in Brazilian understory leaves (R^2 increased from 0.73 to 0.82 and RMSE decreased from 72 days to 60 days; Fig. 9), at the small expense of model performance for Brazilian canopy shade leaves (R^2 decreased from 0.89 to 0.88 and RMSE increased from 48 days to 49 days; Fig. 9).

4. Discussion

We investigated whether principles of leaf trait ecology and ontogeny could be used to create a general model relating leaf spectra to leaf age, taking into account the effect of growth environments. We divided this investigation into two broad questions: (1) How are leaf traits and spectra related to leaf development across different sites and canopy growth environments? (2) Are these relationships sufficiently consistent to allow a general model to accurately predict leaf age from spectra across sites and various canopy environments?

I. How are leaf traits and spectra related to leaf development across different sites and canopy growth environments?

Two key findings address this question:

1. Variation in leaf traits and spectra across all leaves is large compared to datasets that focus only on sunlit mature leaves. Our 759 leaves from 11 trees in Brazil encompassed variation in LMA (35-270 g/m^2), LWC (42-83%) and NIR reflectance (0.35-0.64) (Table S1) that covers over 98% LMA values and 89% NIR reflectance values recorded for the much larger dataset of 1,449 tree species (6,136 leaves) in Asner *et al* (2011, 2014). These results are consistent with those reported at the contrasting forest site with very different soil condition (Quesada *et al.*, 2012) in Peru (Chavana-Bryant *et al.*, 2016) and show that such large variation in traits and spectra can be attributed primarily to the substantial variation across leaf ages (Figs. 2,3) and canopy environments (Figs. 2,3, and S4).

This finding highlights two important points: First, it emphasizes how leaf ages (Hulshof *et al*., 2013; Chavana-Bryant *et al.*, 2016) and canopy environments (Wright *et al*., 2004; Asner *et al*., 2011, 2014; Serbin *et al.*, 2014) can be key drivers of trait variation that cause within-species traits to vary as much or more than variations across species; and second, most relevant for this study, it confirms that if leaf age varies in concert with leaf traits and spectra, then sampling leaves of a broad range of traits (and how they vary with leaf age and canopy environments) may be more important than sampling many sites or species in developing a general model for predicting leaf age from spectra.

2. Leaf traits and spectra vary with both age and canopy environments (Figs. 2,3,6; Fig. S4): Previous studies have found that leaf age influences leaf traits and spectra (Field & Mooney,

1983; Kitajima *et al*., 1997, 2002; Roberts *et al.*, 1998; Wilson *et al*., 2001; Yang *et al*., 2014; Chavana-Bryant *et al.*, 2016) and that canopy environments influence leaf traits (e.g. Lichtenthaler *et al.*, 1981; Givnish *et al.*, 1988; Ellsworth & Reich, 1993; Terashima *et al.*, 2001; Koike *et al*., 2001; Kumagai *et al*., 2001; Cavaleri *et al*., 2010; Kenzo *et al*., 2015; Coble & Cavaleri, 2015), but this study also finds that understanding their interaction (Fig 2, Fig 3a,b) is particularly important for developing general relationships between leaf ages and trait-mediated spectra.

These interacting trait-age and trait-environment relationships lay the foundation for addressing our second question (below). This is because the age-dependent and/or environment-dependent changes in the above-mentioned leaf traits and other related leaf morphological, structural and physico-chemical traits are known to influence leaf optical properties (Curran, 1989; Carter *et al*., 1989; Elvidge, 1990; Jacquemoud & Baret, 1990; Kokaly *et al*., 2009; Asner *et al.*, 2011, 2014; Serbin *et al.*, 2012, 2014; Yang *et al.*, 2014; Chavana-Bryant *et al.*, 2016). Intriguingly, the spectrally-based species identification study of Lang *et al* (2015) noted a result that leaves from young and adult plants differed consistently in their near-infrared spectra, which parallels what we investigated here (and also reported in Chavana-Bryant *et al*., 2016) across the developmental stages of individual leaves within adults. This suggests that, ultimately, the spectra-age relationship in leaves may integrate effects of both individual leaf and whole plant ontogenies.

II. Are these relationships sufficiently consistent to allow a general model to accurately predict leaf age from spectra across sites and various canopy environments?

In general, we find that the answer to this question is yes, as leaf traits (co-varying with leaf spectra) are evidently constrained by ontogenetic physiology and canopy environments. Therefore, leaf traits and spectra vary systematically and predictably with leaf age between forest sites thousands of kilometers apart and across canopy growth environments. This result emerges from two key findings:

1. A single model, developed to predict leaf age from the spectra of sunlit leaves in a southwestern Amazon forest in Peru, predicts sunlit and shade canopy leaf ages from a central eastern Amazon forest in Brazil almost as well without recalibration. The success of the model

537 of Chavana-Bryant *et al* (2016) in predicting ages of sunlit and shade canopy leaves across
538 widely separated sites (Fig. 4a,b) suggests that general rules constrain ontogenic development
539 within similar growth environments. This is also true across all tropical leaves (see finding 2,
540 below) once the differences between canopy environments and associated environment-trait
541 linkages are accounted for (Figs. 2,3). The underlying reason, as discussed before, is that key
542 spectral regions were consistently associated with leaf age (Fig. 3a) and with different growth
543 environments (Fig. 3b).
544
545 *2. Because leaf traits (and hence spectra) vary substantially with growth environments, a more*
546 *general model to accurately predict leaf ages across environments (including both canopy and*
547 *subcanopy trees) can be developed (e.g. by incorporating the samples of wider trait ranges).*
548 Leaf ages predicted by the Peru model deviated from observed ages in a way that
549 systematically and predictably depended on canopy growth environments, developmental
550 pathways and leaf traits (Figs. 5-8). In general, understory leaves exhibited trait values that fell
551 outside the range exhibited by both the Peruvian and Brazilian canopy leaves. Old-leaf traits
552 differed for understory leaves (Fig. 6), and young leaves of some middle-canopy and understory
553 leaves followed a different developmental pathway manifesting reddish color in leaves early in
554 development (Fig. 5). This distinct developmental pathway is possibly a consequence of
555 strategies for herbivore defense in sub-canopy tropical leaves based on delay of chlorophyll
556 infusion in herbivore-abundant environments (Fig. 5a) (Kursar & Coley, 1992; Dominy *et al.*,
557 2002; Queenborough *et al.*, 2013).
558 These observations support the ideas of (a) a model that explicitly included canopy growth
559 environments and leaf traits as new predictor variables alongside leaf spectra (Fig. 9), and (b) a
560 model driven only by leaf spectra, but parameterized by leaves that span the entire trait range
561 found in diverse canopy environments (Fig. 9).
562 Both of these approaches significantly improved model generality, but the spectra-only
563 model, parameterized by leaves across all canopy environments, performed better than one fit to
564 the sun-specific subset of traits. This confirms our hypothesis (H2 from §2.3.3 above) that
565 because spectra are jointly influenced by all leaf traits, whether measured or unmeasured, and
566 therefore this spectral model had more predictive power because it could implicitly account for
567 the effects of unmeasured traits.

We highlight three directions for further work on general leaf-age modeling. First, we note that despite the relatively strong predictive capacity of our recommended "all spectra" leaf age model (Fig. 9c, $R^2 \approx 0.8$ or better), there is still systematic residual variation between predictions of the spectra-age model and observations of leaf age. The residuals of the spectra-age model (Fig. S5) showed a concave nonlinear relationship with observed leaf age, with both young and old leaf ages being under-estimated. This pattern, evident in both Brazil and Peru datasets (Fig S5), suggests that even better models of leaf age may be possible with further work that identifies the causes of this residual variation, and/or through the inclusion of additional leaf variation to expand the range of the modeling approach.

Second, our demonstration here of convergent relations across the broad trait variability induced by both leaf development and growth environments across two distinct forests suggests that even leaf samples from a small set of individuals, if designed to encompass this breadth, may provide a powerful tool to predict leaf developmental trajectories and ages across additional tropical forests, and even forest systems in other biomes. Future studies could use multiple sites, biomes, and plant types to investigate the feasibility of developing general globally-applicable algorithms for leaf age.

Finally, leaf traits and associated spectra evolve with development, but similarly developmental stages may be reached at different ages depending on individuals, canopy environments, and biomes. This suggests that leaves with varying lifespans should be adjusted to a common developmental trajectory (as in Chavana-Bryant *et al*., 2016) in work seeking to generalize models of leaf age to accommodate for leaves with different lifespans. For canopy leaves in Peru versus Brazil, the difference between development-adjusted age (used for Peru leaves by Chavana-Bryant *et al*., 2016) and absolute age (used here for Brazil leaves) was not large, as indicated by the comparably good age model fits for Peru and Brazil canopy leaves (Figs. 4,9). However, middle-canopy and understory leaves can have differences in early developmental pathways (as we have shown for reddish leaves in this study) and can have lifespans several folds longer than canopy leaves (Reich *et al.*, 2004). This implies that for a given absolute age, understory leaves are at an earlier developmental stage, leading to an underestimation of their predicted ages and a decreased in overall model performance when leaves at different developmental stages have the same absolute age. This is evident from the steeper slopes of observed versus predicted age for understory environments compared to other

environments (Fig. 9). We therefore expect that modeling of middle-canopy and understory leaf age would be improved by extending observations of these leaves throughout their life cycle, until senescence (which can take up to several years). We hypothesize that in general, adjusting leaves with varying lifespans to a common developmental trajectory would reveal local (within canopy) to inter-biome convergence in relative leaf aging processes.

5. Conclusion

Our results show the convergent correlations among leaf traits, spectra, and age across various tree species, sites, and growth environments. These results support the development of a general spectra-age model and we have shown that this model can effectively predict leaf age across the observed ontogenic and environmental variation. This study has three important implications for the broader plant science and remote sensing communities.

First, leaf spectra can allow rapid and effective estimation of leaf ages across tropical forests and various canopy environments. Our work, building on previous studies of spectral-leaf traits correlations (Asner *et al.*, 2012, 2014; Serbin *et al*., 2012, 2014) and age-dependence (Chavana-Bryant *et al.*, 2016), shows that reconstructing life cycles of multiple physiochemical properties of leaves across forest sites and canopy environments is possible. Future spectrally-derived studies should give insights into the fundamental mechanisms that regulate the life-cycle of resource investments and return in leaves.

Second, the convergent spectra-age correlation suggests that remotely sensed observations using imaging spectroscopy (also known as “hyperspectral”) data could enable the monitoring and mapping of leaf age compositions across tree crowns and whole landscapes, and provide insights into temporal dynamics of leaf age demography in forest canopies. The generality of these correlations across sites and growth environments also implies that leaf age dependencies of commonly used vegetation indices (VIs) seen at the Peru site (Chavana-Bryant *et al.*, 2016), likely affect these VIs across broad regions. Therefore, remote sensing-based studies of tropical forest seasonality and phenology should account for leaf age effects.

Finally, these findings have important theoretical implications. Leaf traits have been observed to vary substantially over their life cycles, exhibiting as much or more within-species variation than between-species variation in both temperate (McKown *et al.*, 2013; Fajardo & Siefert, 2016) and tropical (Chavana-Bryant *et al.*, 2016) trees. Our extension of this observation

630 across sites and growth environments suggests that fundamental evolutionary rules constrain the
631 co-variations among spectra, traits, and age both within and between species, and that studies
632 that seek insights into these rules (e.g, via analysis of leaf economics, Wright *et al*., 2004; Osnas
633 *et al.*, 2013) should be expanded from their traditional focus on species (generally collected at
634 peak season) to include various leaf developmental stages and their effects on key physiological
635 traits.
636
637 **Acknowledgments**
638 Research in Brazil was supported by NSF (PIRE #0730305), NASA (#NNX11AH24G and
639 NESSF to J.W.), and DOE (GoAmazon #DE-SC0008383). We thank LBA for support, and Dan
640 Metcalfe, Ty Taylor, Kleber Campos, and Katie Berg for assistance. Research in Peru was
641 supported by NERC, via FSF equipment loans and grants to CCH-B (TROBIT project
642 #NE/D005469/1), and to FG via CEH. We thank Olivier Jaudoin, Michael Eltringham, Stefan
643 Curtis, Ana Lombardero Morán, Valentine Alt and Italo Treviño Zeballos for assistance, and
644 Eric Cosio for logistical support in Peru. SPS was supported by the Next-Generation Ecosystem
645 Experiment (NGEE-Tropics) project supported by the U.S. DOE, Office of Science, Office of
646 Biological and Environmental Research and through contract #DE-SC00112704 to Brookhaven
647 National Laboratory.
648
649 **Author contributions**
650 J.W., S.R.S, C.C-B, L.P.A. and S.P.S planned and designed the research. J.W., S.R.S, N.P.,
651 L.P.A., C.C-B, R.C.O. and G.M. designed, performed, and/or supported Brazil field data
652 collection. Data integration and quality assurance at Brazil site were performed by J.W. J.W. and
653 S.P.S designed the Matlab version of PLSR analysis with input from C.C-B. Data analysis was
654 performed by J.W. J.W. wrote the manuscript in close collaboration with S.R.S., with
655 contributions from C.C-B, S.P.S, F.G., Y.M., K.G., X.Y., L.P.A., and W.L.
656

References

Acuna MA, Murphy GE. 2006. Use of near infrared spectroscopy and multivariate analysis to predict wood density of Douglas-fir from chain saw chips. *Forest Prod J.,* **56**: 67-72.

Aho K, Derryberry D, Peterson T. 2014. Model selection for ecologists: the worldviews of AIC and BIC. *Ecology*, **95:** 631-636.

Akaike H. 1974. A new look at the statistical model identification. *Automatic Control, IEEE Transactions on*, **19**: 716-723.

Asner GP, Martin RE. 2011. Canopy phylogenetic, chemical and spectral assembly in a lowland Amazonian forest. *New Phytologist*, **189**: 999-1012.

Asner GP, Martin RE, Tupayachi R, Emerson R, Martinez P, Sinca F, Powell GV, Wright SJ, Lugo AE. 2011. Taxonomy and remote sensing of leaf mass per area (LMA) in humid tropical forests. *Ecological Applications*, **21**: 85-98.

Asner GP, Martin RE, Suhaili AB. 2012. Sources of canopy chemical and spectral diversity in lowland Bornean forest. *Ecosystems*, **15**: 504-517.

Asner GP, Martin RE, Carranza-Jimenez L, Sinca F, Tupayachi R, Anderson CB, Martinez P. 2014. Functional and biological diversity of foliar spectra in tree canopies throughout the Andes to Amazon region. *New Phytologist*, **204**: 127-139.

Bi J, Knyazikhin Y, Choi S, Park T, Barichivich J, Ciais P, Fu R, Ganguly S, Hall F, Hilker T *et al.* 2015. Sunlight mediated seasonality in canopy structure and photosynthetic activity of Amazonian rainforests. *Environmental Research Letters*, **10**: 064014.

Bolster KL, Martin ME, Aber JD. 1996. Determination of carbon fraction and nitrogen concentration in tree foliage by near infrared reflectance: A comparison of statistical methods. *Canadian Journal of Forest Research*, **26**: 590-600.

Brando PM, Goetz SJ, Baccini A, Nepstad DC, Beck PS, Christman MC. 2010. Seasonal and interannual variability of climate and vegetation indices across the Amazon. *Proceedings of the National Academy of Sciences*, **107**: 14685-14690.

Carter GA. 1993. Responses of leaf spectral reflectance to plant stress. *American Journal of Botany*, 239-243.

Cavaleri MA, Oberbauer SF, Clark DB, Clark DA, Ryan MG. 2010. Height is more important than light in determining leaf morphology in a tropical forest. *Ecology*, **91**: 1730-1739.

Chavana-Bryant C, Malhi Y, Wu J, Asner GP, Anatasiou A, Enquist BJ, Saleska SR, Doughty C, Gerard F. Leaf aging of Amazonian canopy trees revealed by spectral and physiochemical measurements. *New Phytologist*, **doi:** 10.1111/nph.13853

Chen CC, Chen H, Chen YR. 2009. A new method to measure leaf age: leaf measuring-interval index. *American journal of botany*, **96**: 1313-1318.

Clark ML, Roberts DA, Clark DB. 2005. Hyperspectral description of tropical rain forest tree species at leaf to crown scales. *Remote Sensing of Environment,* **96**: 375-398.

Coble AP, Cavaleri MA. 2015. Light acclimation optimizes leaf functional traits despite height-related constraints in a canopy shading experiment. *Oecologia*, **177**: 1131-1143.

Coley PD. 1980. Effects of leaf age and plant life history patterns on herbivory. *Nature,* **284**: 545-546.

Coley PD, Barone JA. 1996. Herbivory and plant defenses in tropical forests. *Annual review of ecology and systematics*, 305-335.

Curran PJ. 1989. Remote sensing of foliar chemistry. *Remote sensing of Environment*, **30**: 271-278.

Davidson EA, de Araújo AC, Artaxo P, Balch JK, Brown IF, Bustamante MM, Coe MT, DeFries RS, Keller M, Longo M *et al.* 2012. The Amazon basin in transition. *Nature*, **481**: 321-328.

Dillen SY, de Beeck MO, Hufkens K, Buonanduci M, Phillips NG. 2012. Seasonal patterns of foliar reflectance in relation to photosynthetic capacity and color index in two co-occurring tree species, Quercus rubra and Betula papyrifera. *Agricultural and forest meteorology*, **160**: 60-68.

Doughty CE, Goulden ML. 2008. Seasonal patterns of tropical forest leaf area index and CO2 exchange. *Journal of Geophysical Research: Biogeosciences (2005–2012)*, *113*(G1).

Durgante FM, Higuchi N, Almeida A, Vicentini A. 2013. Species Spectral Signature: Discriminating closely related plant species in the Amazon with Near-Infrared Leaf-Spectroscopy. *Forest Ecol Manag,* **209**: 240-248.

Ellsworth DS, Reich PB. 1993. Canopy structure and vertical patterns of photosynthesis and related leaf traits in a deciduous forest**.** *Oecologia,* **96**: 169-178.

Elvidge CD. 1990. Visible and near infrared reflectance characteristics of dry plant materials. *Remote Sensing*, **11**: 1775-1795.

Erickson RO, Michelini FJ. 1957. The plastochron index. *American Journal of Botany*, 297-305.

Fajardo A, Siefert A. 2016. Phenological variation of leaf functional traits within species. *Oecologia*: 1-9.

Field C. 1983. Allocating leaf nitrogen for the maximization of carbon gain: leaf age as a control on the allocation program. *Oecologia*, **56**: 341-347.

Field C, Mooney HA. 1983. Leaf age and seasonal effects on light, water, and nitrogen use efficiency in a California shrub. *Oecologia*, **56**: 348-355.

Funk JL, Cornwell WK. 2013. Leaf traits within communities: context may affect the mapping of traits to function. *Ecology*, **94**: 1893-1897.

Gamon JA, Penuelas J, Field CB. 1992. A narrow-waveband spectral index that tracks diurnal changes in photosynthetic efficiency. *Remote Sensing of environment*, **41**: 35-44.

Gao BC. 1996. NDWI—a normalized difference water index for remote sensing of vegetation liquid water from space. *Remote sensing of environment*, **58**: 257-266.

Geladi P, Kowalski BR. 1986. Partial least-squares regression: a tutorial. *Analytica chimica acta*, **185**: 1-17.

Givnish TJ. 1988. Adaptation to sun and shade: a whole-plant perspective.*Functional Plant Biology*, **15**: 63-92.

Grossman YL, Ustin SL, Jacquemoud S, Sanderson EW, Schmuck G, Verdebout J. 1996. Critique of stepwise multiple linear regression for the extraction of leaf biochemistry information from leaf reflectance data. *Remote Sensing of Environment,* **56**: 182-193.

Huete AR, Didan K, Miura T, Rodriguez EP, Gao X, Ferreira LG. 2002. Overview of the radiometric and biophysical performance of the MODIS vegetation indices. *Remote Sensing of Environment,* **83**: 195-213.

Hulshof CM, Violle C, Spasojevic MJ, McGill B, Damschen E, Harrison S, Enquist B. 2013. Intra-specific and inter-specific variation in specific leaf area reveal the importance of abiotic and biotic drivers of species diversity across elevation and latitude. *Journal of Vegetation Science*, **24**: 921-931.

748 **Hutyra LR, Munger JW, Saleska SR, Gottlieb E, Daube BC, Dunn AL, Amaral DF, de**
749 **Camargo PB, Wofsy SC.** 2007. Seasonal controls on the exchange of carbon and water
750 in an Amazonian rain forest. *Journal of Geophysical Research: Biogeosciences (2005–*
751 *2012)*, *112*(G3).
752 **Jacquemoud S, Baret F.** 1990. PROSPECT: A model of leaf optical properties spectra. *Remote*
753 *sensing of environment*, **34**: 75-91.
754 **Jiang Z, Huete AR, Didan K, Miura T.** 2008. Development of a two-band enhanced
755 vegetation index without a blue band. *Remote Sensing of Environment*, **112**: 3833-3845.
756 **Keenan TF, Darby B, Felts E, Sonnentag O, Friedl MA, Hufkens K, O'Keefe J, Klosterman**
757 **S, Munger JW, Richardson AD.** 2014. Tracking forest phenology and seasonal
758 physiology using digital repeat photography: a critical assessment. *Ecological*
759 *Applications*, **24**: 1478-1489.
760 **Kenzo T, Inoue Y, Yoshimura M, Yamashita M, Tanaka-Oda A, Ichie T.** 2015. Height-
761 related changes in leaf photosynthetic traits in diverse Bornean tropical rain forest trees.
762 *Oecologia*, **177**: 191-202.
763 **Kitajima K, Mulkey SS, Wright SJ.** 1997. Decline of photosynthetic capacity with leaf age in
764 relation to leaf longevities for five tropical canopy tree species.*American Journal of*
765 *Botany*, **84**: 702-702.
766 **Kitajima K, Mulkey SS, Samaniego M, Wright SJ.** 2002. Decline of photosynthetic capacity
767 with leaf age and position in two tropical pioneer tree species. *American Journal of*
768 *Botany*, **89**: 1925-1932.
769 **Koike T, Kitao M, Maruyama Y, Mori S, Lei TT.** 2001. Leaf morphology and photosynthetic
770 adjustments among deciduous broad-leaves trees within the vertical canopy profile. *Tree*
771 *Physiology,* **21**: 951-958.
772 **Kokaly RF, Asner GP, Ollinger SV, Martin ME, Wessman CA.** 2009. Characterizing canopy
773 biochemistry from imaging spectroscopy and its application to ecosystem studies. *Remote*
774 *Sensing of Environment*, **113**: S78-S91.
775 **Kramer K, Leinonen I, Loustau D.** 2000. The importance of phenology for the evaluation of
776 impact of climate change on growth of boreal, temperate and Mediterranean forests
777 ecosystems: an overview. *International Journal of Biometeorology*, **44**: 67-75.
778 **Kumagai TO, Kuraji K, Noguchi H, Tanaka Y, Tanaka K, Suzuki M.** 2001. Vertical profiles
779 of environmental factors within tropical rainforest, Lambir Hills National Park, Sarawak,
780 Malaysia. *Journal of Forest Research*, **6**: 257-264.
781 **Kursar TA, Coley PD.** 1992. Delayed greening in tropical leaves: an antiherbivore defense?.
782 *Biotropica*, **24**: 256-262.
783 **Lang C, Costa FRC, Camargo JLC, Durgante FM, Vicentini A.** 2015. Near infrared
784 spectroscopy facilitates rapid identification of both young and mature Amazonian tree
785 species. *PLOS One*, **10**: e0134521.
786 **Lawrence R, Potts BM, Whitham TG**. 2003. Relative importance of plant ontogeny, host
787 genetic variation, and leaf age for a common herbivore. *Ecology*, **84**: 1171-1178.
788 **Lewis SL, Brando PM, Phillips OL, van der Heijden GM, Nepstad D.** 2011. The 2010
789 amazon drought. *Science*, **331**: 554-554.
790 **Lichtenthaler HK, Buschmann C, Döll M, Fietz HJ, Bach T, Kozel U, Meier D, Rahmsdorf**
791 **U.** 1981. Photosynthetic activity, chloroplast ultrastructure, and leaf characteristics of
792 high-light and low-light plants and of sun and shade leaves. *Photosynthesis research*, **2**:
793 115-141.

Luss S, Schwanninger M, Rosner S. 2015. Hydraulic traits of Norway spruce sapwood estimated by Fourier transform near-infrared spectroscopy (FT-NIR). *Canadian Journal of Forest Research,* **45**: 625-631.

Maksymowych R. 1973. *Analysis of leaf development* (No. 1). CUP Archive.

Malhi Y, Phillips OL, Lloyd J, Baker T, Wright J, Almeida S, Arroyo L, Frederiksen T, Grace J, Higuchi N *et al.* 2002. An international network to monitor the structure, composition and dynamics of Amazonian forests (RAINFOR). *Journal of Vegetation Science*, **13**: 439-450.

Malhi Y, Wood D, Baker TR, Wright J, Phillips OL, Cochrane T, Meir P, Chave J, Almeida S, Arroyo L, *et al.* 2006. The regional variation of aboveground live biomass in old-growth Amazonian forests. *Global Change Biology*, **12:** 1107-1138.

Malhi Y, Amézquita F, Doughty C E, Silva-Espejo JE, Girardin CA, Metcalfe DB, Aragao LEOC, Huaraca-Quispe LP, Alzamora-Taype I, Eguiluz-Mora L *et al.* 2014. The productivity, metabolism and carbon cycle of two lowland tropical forest plots in south-western Amazonia, Peru. *Plant Ecology & Diversity*, **7**: 85-105.

McKown AD, Guy RD, Azam MS, Drewes EC, Quamme LK. 2013. Seasonality and phenology alter functional leaf traits. *Oecologia* **172**(3): 653-665.

Meicenheimer RD. 2014. The plastochron index: Still useful after nearly six decades. *American journal of botany*, **101**: 1821-1835.

Morton DC, Nagol J, Carabajal CC, Rosette J, Palace M, Cook BD, Vermote EF, Harding JD, North PR. 2014. Amazon forests maintain consistent canopy structure and greenness during the dry season. *Nature*, **506**: 221-224.

Nilson T, Pisek J, Rautiainen M, Peterson U. 2012. *Seasonal reflectance courses of forests*. INTECH Open Access Publisher.

Osnas JL, Lichstein JW, Reich PB, Pacala SW. 2013. Global leaf trait relationships: mass, area, and the leaf economics spectrum. *Science*, **340**: 741-744.

Opler PA, Frankie GW, Baker HG. 1980. Comparative phenological studies of treelet and shrub species in tropical wet and dry forests in the lowlands of Costa Rica. *The Journal of Ecology*, 167-188.

Otsu N. 1975. A threshold selection method from gray-level histograms. *Automatica*, **11**: 23-27.

Pantin F, Simonneau T, Muller B. 2012. Coming of leaf age: control of growth by hydraulics and metabolics during leaf ontogeny. *New Phytologist*, **196**: 349-366.

Patiño S, Lloyd J, Paiva R, Baker TR, Quesada CA, Mercado LM, Schmerler J, Schwarz M, Santos AJB, Aguilar A, *et al.* 2009. Branch xylem density variations across the Amazon Basin. *Biogeosciences*, **6:** 545-568.

Petisco C, Garcia-Criado B, Mediavilla S, de Aldana BRV, Zabalgogeazcoa I, Garcia-Ciudad A. 2006. Near-infrared reflectance spectroscopy as a fast and non-destructive tool to predict foliar organic constituents of several woody species. *Analytical and Bioanalytical Chemistry* **386**: 1823-1833.

Queenborough SA, Metz MR, Valencia R, Wright SJ. 2013. Demographic consequences of chromatic leaf defence in tropical tree communities: do red young leaves increase growth and survival?. *Annals of botany*, **112**: 677-684.

Quesada CA, Lloyd J, Schwarz M, Patino S, Baker TR, Czimczik C, Fyllas NM, Martinelli L, Nardoto GB, Schmerler J *et al.* 2010. Variations in chemical and physical properties of Amazon forest soils in relation to their genesis. *Biogeosciences*, **7**: 1515-1541.

Quesada CA, Phillips OL, Schwarz M, Czimczik CI, Baker TR, Patino S, Fyllas NM, Hodnett MG, Herrera R, Almeida S, *et al.* 2012. Basin-wide variations in Amazon forest structure and function are mediated by both soils and climate. *Biogeosciences*, **9:** 2203-2246.

Ramirez JA, Posada JM, Handa IT, Hoch G, Vohland M, Messier C, Reu B. 2015. Near-infrared spectroscopy (NIRS) predicts non-structural carbohydrate concentrations in different tissue types of a broad range of tree species. *Methods in Ecology and Evolution*, **6**, 1018-1025

Reich PB, Walters MB, Ellsworth DS. 1991. Leaf age and season influence the relationships between leaf nitrogen, leaf mass per area and photosynthesis in maple and oak trees. *Plant, Cell & Environment*, **14**: 251-259.

Reich PB, Walters MB, Ellsworth DS. 1992. Leaf life-span in relation to leaf, plant, and stand characteristics among diverse ecosystems. *Ecological monographs*, **62**: 365-392.

Reich PB. 1995. Phenology of tropical forests: patterns, causes, and consequences. *Canadian Journal of Botany*, **73**: 164-174.

Reich PB, Walters MB, Ellsworth DS. 1997. From tropics to tunda: global convergence in plant functioning. *Proceedings of the National Academy of Sciences,* **94**: 13730-13734.

Reich PB, Uhl C, Walters MB, Prugh L, Ellsworth DS. 2004. Leaf demography and phenology in Amazonian rain forest: a census of 40 000 leaves of 23 tree species. *Ecological Monographs*, **74**: 3-23.

Restrepo-Coupe N, da Rocha HR, Hutyra LR, da Araujo AC, Borma LS, Christoffersen B, Cabral OMR, de Camargo PB, Cardoso FL, da Costa ACL *et al.* 2013. What drives the seasonality of photosynthesis across the Amazon basin? A cross-site analysis of eddy flux tower measurements from the Brasil flux network. *Agricultural and forest meteorology*, **182**: 128-144.

Rice AH, Pyle EH, Saleska SR, Hutyra L, Palace M, Keller M, de Camargo PB, Portilho K, Marques DF, Wofsy SC. 2004. Carbon balance and vegetation dynamics in an old-growth Amazonian forest. *Ecological Applications*, **14**: 55-71.

Richardson AD, Braswell BH, Hollinger DY, Jenkins JP, Ollinger SV. 2009. Near-surface remote sensing of spatial and temporal variation in canopy phenology. *Ecological Applications*, **19**: 1417-1428.

Richardson AD, Anderson RS, Arain MA, Barr AG, Bohrer G, Chen G, Chen JM, Ciais P, Davis KJ, Desai AR, *et al.* 2012. Terrestrial biosphere models need better representation of vegetation phenology: results from the North American Carbon Program Site Synthesis. *Global Change Biology*, **18**: 566-584.

Roberts DA, Nelson BW, Adams JB, Palmer F. 1998. Spectral changes with leaf aging in Amazon caatinga. *Trees*, **12**: 315-325.

Saleska, S.R., J. Wu, K. Guan, A.C. Araujo, A. Huete, A.D. Nobre, N. Restrepo-Coupe. 2016. Brief Communications Arising: Dry season greening of Amazon forests. *Nature*, **531:** E4-E5.

Schöngart J, Piedade MTF, Ludwigshausen S, Horna V, Worbes M. 2002. Phenology and stem-growth periodicity of tree species in Amazonian floodplain forests. *Journal of Tropical Ecology*, **18**: 581-597.

Sellers PJ, Berry JA, Collatz GJ, Field CB, Hall FG. 1992. Canopy reflectance, photosynthesis, and transpiration. III. A reanalysis using improved leaf models and a new canopy integration scheme. *Remote Sensing of Environment*, **42:** 187-216

885 **Serbin SP, Dillaway DN, Kruger EL, Townsend PA.** 2012. Leaf optical properties reflect
886 variation in photosynthetic metabolism and its sensitivity to temperature. *Journal of*
887 *Experimental Botany*, **63**: 489-502.
888 **Serbin SP, Singh A, McNeil BE, Kingdon CC, Townsend PA.** 2014. Spectroscopic
889 determination of leaf morphological and biochemical traits for northern temperate and
890 boreal tree species. *Ecological Applications*, **24**: 1651-1669.
891 **Singh A, Serbin SP, McNeil BE, Kingdon CC, Townsend PA.** 2015. Imaging spectroscopy
892 algorithms for mapping canopy foliar chemical and morphological traits and their
893 uncertainties. *Ecological Applications*, **25:** 2180-2197.
894 **Terashima I, Miyazawa SI, Hanba YT.** 2001. Why are sun leaves thicker than shade leaves?—
895 Consideration based on analyses of CO2 diffusion in the leaf. *Journal of Plant Research,*
896 **114**: 93-105.
897 **Toomey M, Roberts D, Nelson B.** 2009. The influence of epiphylls on remote sensing of humid
898 forests. *Remote Sensing of Environment*, **113**: 1787-1798.
899 **Townsend PA, Foster JR, Chastain RA, Currie WS.** 2003. Application of imaging
900 spectroscopy to mapping canopy nitrogen in the forests of the central Appalachian
901 Mountains using Hyperion and AVIRIS. *IEEE Transactions on Geoscience and Remote*
902 *Sensing*, **41**: 1347-1354.
903 **Tucker CJ.** 1979. Red and photographic infrared linear combinations for monitoring vegetation.
904 *Remote Sensing of Environment*, **8**: 127-150.
905 **Ustin SL, Gitelson AA, Jacquemoud S, Schaepman M, Asner GP, Gamon JA, Zarco-**
906 **Tejada P.** 2009. Retrieval of foliar information about plant pigment systems from high
907 resolution spectroscopy. *Remote Sensing of Environment*, **113**: S67-S77.
908 **Wang Y, Siemann E, Wheeler GS, Zhu L, Gu X, Ding J.** 2012. Genetic variation in anti-
909 herbivore chemical defences in an invasive plant. *Journal of Ecology*, **100**: 894-904.
910 **Wilson KB, Baldocchi DD, Hanson PJ.** 2001. Leaf age affects the seasonal pattern of
911 photosynthetic capacityand net ecosystem exchange of carbon in a deciduous forest.
912 *Plant, Cell & Environment*, **24**: 571-583.
913 **Wolter PT, Townsend PA, Sturtevant BR, Kingdon CC.** 2008. Remote sensing of the
914 distribution and abundance of host species for spruce budworm in Northern Minnesota
915 and Ontario. *Remote Sensing of Environment*, **112**: 3971-3982.
916 **Wold S, Sjöström M, Eriksson L.** 2001. PLS-regression: a basic tool of
917 chemometrics. *Chemometrics and intelligent laboratory systems*, **58**: 109-130.
918 **Wright IJ, Reich PB, Westoby M, Ackerly DD, Baruch Z, Bongers F, Cavender-Bares J,**
919 **Chapin T, Cornelissen JHC, Diemer M, *et al.*** (2004). The worldwide leaf economics
920 spectrum. *Nature*, **428**: 821-827.
921 **Xu QS, Liang YZ.** 2001. Monte Carlo cross validation. *Chemometrics and Intelligent*
922 *Laboratory Systems*, **56**: 1-11.
923 **Yang X, Tang J, Mustard JF.** 2014. Beyond leaf color: Comparing camera-based phenological
924 metrics with leaf biochemical, biophysical, and spectral properties throughout the
925 growing season of a temperate deciduous forest. *Journal of Geophysical Research:*
926 *Biogeosciences*, **119**: 181-191.
927 **Wu J, Albert LP, Lopes AP, Restrepo-Coupe N, Hayek M, Wiedemann K, Guan K, Stark**
928 **SC, Christoffersen B, Prohaska N, *et al.*** 2016. Leaf development and demography
929 explain photosynthetic seasonality in Amazonian evergreen forests. *Science*, **351**: 972-
930 976.

Table 1. Tree-environment combinations and associated canopy environments for leaf traits and spectra measurements at two tropical forests in Brazil and Peru. (Tree-environment combinations were coded by *"species name_canopy position"*, with four canopy position codes: 'SU' sunlit, 'SH' shaded, 'MC' mid-canopy, and 'US' understory).

Field Site	Tree-environment combination	Species	Family	DBH (m)	Canopy Position	Branch Height (m)	Branch Depth (m)	Old LMA (g/m^2)	Old LWC (%)
Brazil	*E. uncinatum* _SU	*Erisma uncinatum Warm.*	Vochysiaceae	1.48	Canopy Sun	39.0	1.0	192.60	49.63
Brazil	*E. uncinatum* _SH	*Erisma uncinatum Warm.*	Vochysiaceae	1.48	Canopy Shade	30.0	10.0	130.79	48.33
Brazil	*Ocotea sp* _SU	*Ocotea sp.*	Lauraceae	0.73	Canopy Sun	37.0	1.0	131.37	47.57
Brazil	*Ocotea sp* _SH	*Ocotea sp.*	Lauraceae	0.73	Canopy Shade	32.5	5.5	91.17	45.28
Brazil	*M.huberi* _SU	*Manilkara huberi (Ducke) A. Chev.*	Sapotaceae	0.92	Canopy Sun	37.5	0.5	229.94	49.18
Brazil	*M.huberi* _SH	*Manilkara huberi (Ducke) A. Chev.*	Sapotaceae	0.92	Canopy Shade	31.2	6.8	218.25	50.39
Brazil	*C.scleroxylon* _SU	*Chamaecrista scleroxylon (Ducke) H.S.Irwin & Barneby*	Leguminosae-Caesalpinioideae	0.47	Canopy Sun	24.5	1.0	80.47	49.79
Brazil	*C.scleroxylon* _SH	*Chamaecrista scleroxylon (Ducke) H.S.Irwin & Barneby*	Leguminosae-Caesalpinioideae	0.47	Canopy Shade	20.0	5.5	59.31	55.74
Brazil	*E.uchi*_MC	*Endopleura uchi (Huber) Cuatrec.*	Humiriaceae	0.46	Middle Canopy	24.5	16.5	114.19	46.01
Brazil	*E.coriacea*_MC	*Eschweilera coriacea*	Lecythidaceae	0.25	Middle Canopy	22.8	15.2	122.01	44.63
Brazil	*H.courbaril*_MC	*Hymenaea courbaril L.*	Leguminosae-Caesalpinioideae	0.45	Middle Canopy	30.0	11.0	117.21	52.02
Brazil	*Miconia sp*_US	*Miconia-sp.*	Melastomataceae	0.14	Understory	13.7	29.3	58.62	61.37
Brazil	*G.amazonicum*_US	*Glycydendron amazonicum (Ducke)*	Euphorbiaceae	0.11	Understory	7.7	33.3	54.74	62.96
Brazil	*M.ruficalyx*_US	*Miconia ruficalyx Gleason*	Melastomataceae	0.14	Understory	13.5	12.0	54.73	59.8
Brazil	*V. elongate*_US	*Virola elongata (Benth.) Warb.*	Myristicaceae	0.17	Understory	19.0	6.5	75.65	59.84
Peru	*L.brittoniana*_SU	*Licania brittoniana*	Chrysobalanaceae	1.88	Canopy Sun	29.5	0.5	121.09	49.89
Peru	*Q.simaruba*_SU	*Quassia simaruba*	Simaroubaceae	1.62	Canopy Sun	29.0	0.5	188.04	44.49
Peru	*R.ovale*_SU	*Ruizodendron ovale*	Annonaceae	1.23	Canopy Sun	32.6	0.5	91.27	50.53
Peru	*A.parvifolium*_SU	*Aspidosperma parvifolium*	Apocynaceae	1.57	Canopy Sun	33.7	0.5	110.94	55.09
Peru	*C.macrosperma*_SU	*Couratari macrosperma*	Lecythidaceae	1.43	Canopy Sun	33.7	0.5	170.65	45.78
Peru	*L.longistyla*_SU	*Licania longistyla*	Chrysobalanacea	1.43	Canopy Sun	30.3	0.5	125.87	37.70
Peru	*B.excelsa*_SU	*Bertholletia excelsa*	Lecythidaceae	2.30	Canopy Sun	34.0	0.5	147.93	45.07
Peru	*T.chrysaloides*_SU	*Tachigali chrysaloides*	Caesalpinioideae	2.10	Canopy Sun	29.7	0.5	180.51	47.29
Peru	*C.racemosa*_SU	*Clarisia racemosa*	Moraceae	1.58	Canopy Sun	33.8	0.5	120.86	49.76
Peru	*E.coriacea*_SU	*Eschweilera coriacea*	Lecythidaceae	1.88	Canopy Sun	33.3	0.5	157.55	46.61
Peru	*G.boliviana*_SU	*Gautteria boliviana*	Annonaceae	1.17	Canopy Sun	31.9	0.5	113.31	52.22
Peru	*P.franciscana*_SU	*Pouteria franciscana*	Sapotacea	2.37	Canopy Sun	35.4	0.5	124.72	48.31

DBH, diameter at breast height; LMA, leaf mass per area; LWC, leaf water content; Old: leaf age greater than 300 days (and senescent leaves were excluded).

939 **Figure Legends**

940 **Figure 1.** Location of sites in the Amazon basin, including the Tapajos National Forest in Brazil
941 (red circle) and the Tambopata National Reserve in Peru (red triangle). The black curve indicates
942 the boundary of the Amazon basin. The background is a map of dry season length (in months;
943 see color legend), which is derived from Tropical Rainfall Measuring Mission (TRMM) satellite
944 data from 1998 to 2013.
945
946 **Figure 2.** Leaf trait variation with leaf age and canopy environment at the Brazil site for 11 tree-
947 environment combinations (see Table 1): **(a)** Leaf Mass per Area (LMA), and **(b)** Leaf Water
948 Content (LWC). Each colored line represents a tree in a particular environment (indicated by a
949 *"species name_canopy position"* label in the legend, where "canopy position" is represented by
950 four codes: 'SU' sunlit, 'SH' shaded, 'MC' mid-canopy, and 'US' understory). Solid colored
951 lines indicate canopy sunlit environment (R^2=0.31 for LMA and R^2=0.60 for LWC) and canopy
952 shade environment (R^2=0.23 for LMA and R^2=0.80 for LWC), dashed lines indicate mid-canopy
953 (MC, R^2=0.76 for LMA and R^2=0.74 for LWC) or understory (US, R^2=0.39 for LMA and
954 R^2=0.61 for LWC), and black lines indicate community average relationships: R^2 is the
955 proportion of variation in the trait that is explained by leaf age (model: log(trait) = a * log(age)
956 +b). *** indicates $p<10^{-5}$.
957
958 **Figure 3.** Leaf age and canopy environment induced spectra variation at the Brazil site. **(a)** Age-
959 dependent leaf level hyperspectral reflectance across all canopy environments for: young (blue
960 lines), mature (green lines), and old (red lines) leaves (mean value in solid lines with shaded 95%
961 confidence interval); **(b)** Canopy environment-dependent leaf level hyperspectral reflectance
962 across all leaf ages for: canopy sun (in red lines; n=4 trees), canopy shade (in purple lines; n=4),
963 mid-canopy (in green lines; n=3), and understory (in blue lines; n=4); **(c)** Normalized differences
964 of young, mature, and old leaf spectra from the mean leaf spectra (solid lines +/- shaded 95%
965 confidence interval); **(d)** Normalized environment differences of canopy sun, canopy shade, mid-
966 canopy and understory leaf spectra from the mean leaf spectra (solid lines +/- shaded 95%
967 confidence interval). Note: Normalized difference = (mean reflectance within age scenario –
968 mean reflectance across all scenarios)/standard deviation of reflectance across all scenarios.
969

970 **Figure 4.** Cross-site spectra-age model results for data from both Peruvian and Brazilian sites,
971 based on fitting variation of the Peru reference Partial Least Squares Regression (PLSR) models
972 to a subset of observations at the Peru site only (i.e., the Peru training dataset): **(a):** Root Mean
973 Square Error (RMSE) between observed and modeled leaf age plotted against the number of
974 latent variables incorporated for PLSR models; **(b):** The proportion of variation in leaf age
975 explained by PLSR models **(**R^2) plotted against the number of latent variables incorporated.
976 Different symbols in (a) and (b) represent different datasets, as indicated (see also Table 1): the
977 performance of the original 7-latent variable model for each dataset is indicated by the points in
978 the blue shaded box in **a, b)**; an optimal model for prediction across sites (RMSE minimized and
979 R^2 maximized for Brazil validation datasets not used in model fitting) emerges for 5 latent
980 variables (gray shaded box in **a, b**). **(c):** Spectral regression coefficients for the optimized PLSR
981 model with 5 latent variables; **(d):** Variable Importance in Projection (VIP) for the optimized
982 PLSR model with 5 latent variables (spectral features greater than 0.8 represent the important
983 spectral regions for leaf age modeling).
984
985 **Figure 5.** Example of developmental trajectory in a mid-canopy tree in Brazil (*E.uchi*_MC),
986 including: **(a)** the appearance of leaves versus age in RGB photos, showing reddish leaves when
987 leaf ages are 40 days or younger; **(b)** the aging of leaves as revealed by leaf reflectance
988 hyperspectra (measured by an ASD spectradiometer); and **(c)** comparison between spectra-age
989 model coefficients of seven latent variables (in red) and five latent variables (in black), (see Fig.
990 4; as derived from the model parameterized by Peruvian sunlit canopy leaves, which do not have
991 reddish young leaves). Coefficients in the spectral region marked by the blue window are near-
992 zero in the 5-variable model, which more accurately predicts leaf age in three mid-canopy or
993 understory trees: (d) *E.uchi*_MC, (e) *G. amazonicum*_US, and (f) *M. ruficalyx*_US). The non-
994 zero coefficients in the 7-variable model make it more sensitive to reddish shifts in the
995 understory Brazilian leaves, a confounding effect which causes significant over-prediction of
996 young leaf age in these same trees when the 7-variable model is applied (in g, h, i).
997
998 **Figure 6. (a)** Branch height probability distribution for Peru (grey line) and Brazil (dark green),
999 with color symbols indicating branch height for each sample; **(b)** Leaf trait scatter plot showing
1000 leaf water content (LWC) versus leaf mass per area (LMA) for Peru and Brazil leaf samples from

1001 the old leaf age class (Table 1). Red rectangles in (a) and (b) bound the sample space for mid- to
1002 upper canopy leaves from Peru and Brazil sites.
1003
1004 **Figure 7.** Performance (observed versus predicted leaf age) of the optimal Peru-trained spectral
1005 leaf age model (Fig 4, 5-variable model) as applied to Brazilian samples from four canopy
1006 environments **(a)-(d):** canopy sun; **(e)-(h)**: canopy shade; **(i)-(k):** mid-canopy; **(l)-(o):** understory.
1007 OLS regressions (black lines) quantify the deviation of the scatterplots from the ideal 1:1 line
1008 (dashed lines). R^2 quantifies the fit of the regression line – i.e., the variation in leaf age explained
1009 by combining the Peru leaf age model (applied to the whole dataset) with the individual tree
1010 regressions – and RMSE is the corresponding Root Mean Square Error.
1011
1012 **Figure 8.** The regression line slopes and intercepts of each tree-environment combination (from
1013 Fig. 7) plotted against branch height and leaf mass per area (LMA) for the Brazil site: **(a)** Slope
1014 vs. branch height; **(b)** Slope vs. LMA; **(c)** Intercept vs. branch height; **(d)** Intercept vs. LMA.
1015
1016 **Figure 9.** Performance of leaf age models for the Brazilian leaf samples under four scenarios: **(a)**
1017 the Peru model (parameterized by using Peruvian leaf spectra only; the same model as presented
1018 in Chavana-Bryant *et al.*, 2016 using seven latent variables); **(b)** the Peru reference model
1019 (parameterized by using Peruvian leaf spectra only); **(c)** the "Peru Spectra+all Trait" model
1020 (parameterized by using Peruvian leaf spectra and traits); **(d)** the "All Spectra" model
1021 (parameterized by using both Brazilian and Peruvian leaf spectra); **(e)** the "All Spectra+ all Trait"
1022 model (or parameterized by using both Brazilian and Peruvian leaf spectra and traits). Four
1023 different color circles represent the leaf samples from Brazil canopy sun (red circles; n=4 trees),
1024 Brazil canopy shade (yellow circles; n=4), Brazil mid-canopy (green circles; n=3), and Brazil
1025 understory trees (blue circles; n=4). Four different color lines represent the corresponding
1026 ordinary least regression (OLS) between predicted and observed leaf ages; central grey line
1027 represents the OLS analysis for all Brazil samples. The "All Spectra" model (d) is our
1028 "recommended" general model. The number of optimal latent variables in panel b was identified
1029 in Fig. 4, and in panels c to e were identified in Fig. S6
1030
1031

Main Figures and Tables

Figure 1. Location of sites in the Amazon basin, including the Tapajos National Forest in Brazil (red circle) and the Tambopata National Reserve in Peru (red triangle). The black curve indicates the boundary of the Amazon basin. The background is a map of dry season length (in months; see color legend), which is derived from Tropical Rainfall Measuring Mission (TRMM) satellite data from 1998 to 2013.

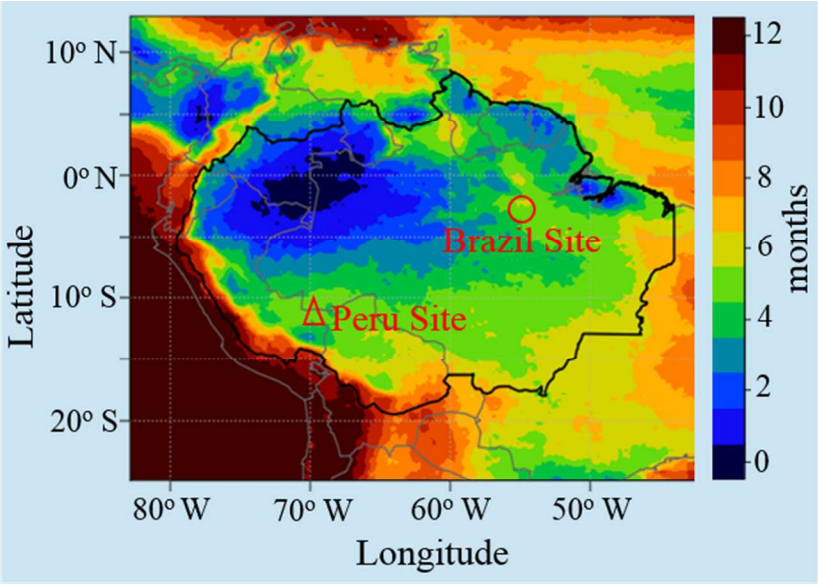

Figure 2. Leaf trait variation with leaf age and canopy environment at the Brazil site for 11 tree-environment combinations (see Table 1): **(a)** Leaf Mass per Area (LMA), and **(b)** Leaf Water Content (LWC). Each colored line represents a tree in a particular environment (indicated by a *"species name_canopy position"* label in the legend, where "canopy position" is represented by four codes: 'SU' sunlit, 'SH' shaded, 'MC' mid-canopy, and 'US' understory). Solid colored lines indicate canopy sunlit environment (R^2=0.31 for LMA and R^2=0.60 for LWC) and canopy shade environment (R^2=0.23 for LMA and R^2=0.80 for LWC), dashed lines indicate mid-canopy (MC, R^2=0.76 for LMA and R^2=0.74 for LWC) or understory (US, R^2=0.39 for LMA and R^2=0.61 for LWC), and black lines indicate community average relationships: R^2 is the proportion of variation in the trait that is explained by leaf age (model: log(trait) = a * log(age) +b). *** indicates $p<10^{-5}$.

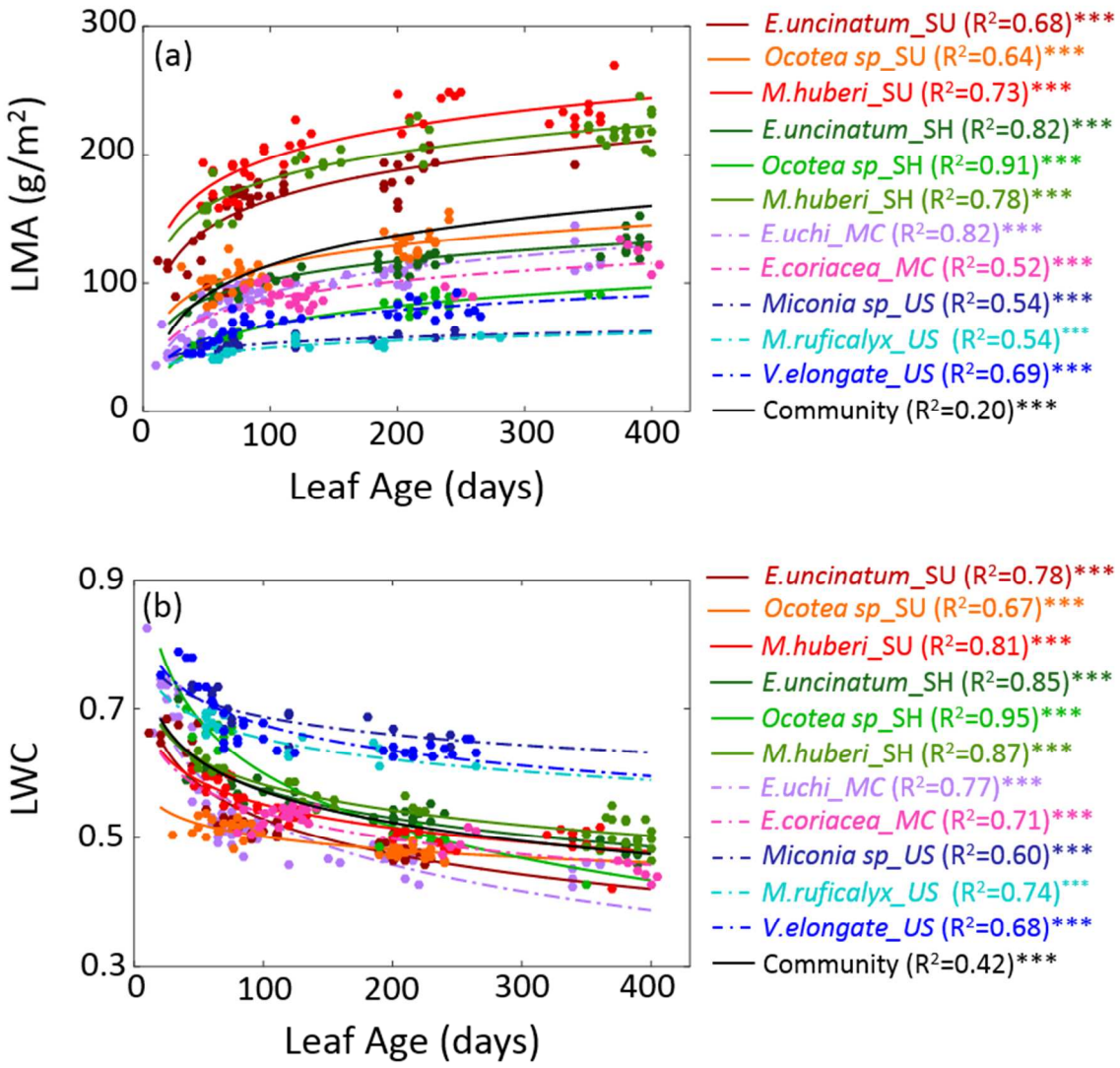
(a)
LMA (g/m²)
300
200
100
0
0
100
200
300
400
Leaf Age (days)
E.uncinatum_SU (R²=0.68)***
Ocotea sp_SU (R²=0.64)***
M.huberi_SU (R²=0.73)***
E.uncinatum_SH (R²=0.82)***
Ocotea sp_SH (R²=0.91)***
M.huberi_SH (R²=0.78)***
E.uchi_MC (R²=0.82)***
E.coriacea_MC (R²=0.52)***
Miconia sp_US (R²=0.54)***
M.ruficalyx_US (R²=0.54)***
V.elongate_US (R²=0.69)***
Community (R²=0.20)***
(b)
LWC
0.9
0.7
0.5
0.3
0
100
200
300
400
Leaf Age (days)
E.uncinatum_SU (R²=0.78)***
Ocotea sp_SU (R²=0.67)***
M.huberi_SU (R²=0.81)***
E.uncinatum_SH (R²=0.85)***
Ocotea sp_SH (R²=0.95)***
M.huberi_SH (R²=0.87)***
E.uchi_MC (R²=0.77)***
E.coriacea_MC (R²=0.71)***
Miconia sp_US (R²=0.60)***
M.ruficalyx_US (R²=0.74)***
V.elongate_US (R²=0.68)***
Community (R²=0.42)***

1052

Figure 3. Leaf age and canopy environment induced spectra variation at the Brazil site. **(a)** Age-dependent leaf level hyperspectral reflectance across all canopy environments for: young (blue lines), mature (green lines), and old (red lines) leaves (mean value in solid lines with shaded 95% confidence interval); **(b)** Canopy environment-dependent leaf level hyperspectral reflectance across all leaf ages for: canopy sun (in red lines; n=4 trees), canopy shade (in purple lines; n=4), mid-canopy (in green lines; n=3), and understory (in blue lines; n=4); **(c)** Normalized differences of young, mature, and old leaf spectra from the mean leaf spectra (solid lines +/- shaded 95% confidence interval); **(d)** Normalized environment differences of canopy sun, canopy shade, mid-canopy and understory leaf spectra from the mean leaf spectra (solid lines +/- shaded 95% confidence interval). Note: Normalized difference = (mean reflectance within each scenario – mean reflectance across all scenarios)/standard deviation of reflectance across all scenarios.

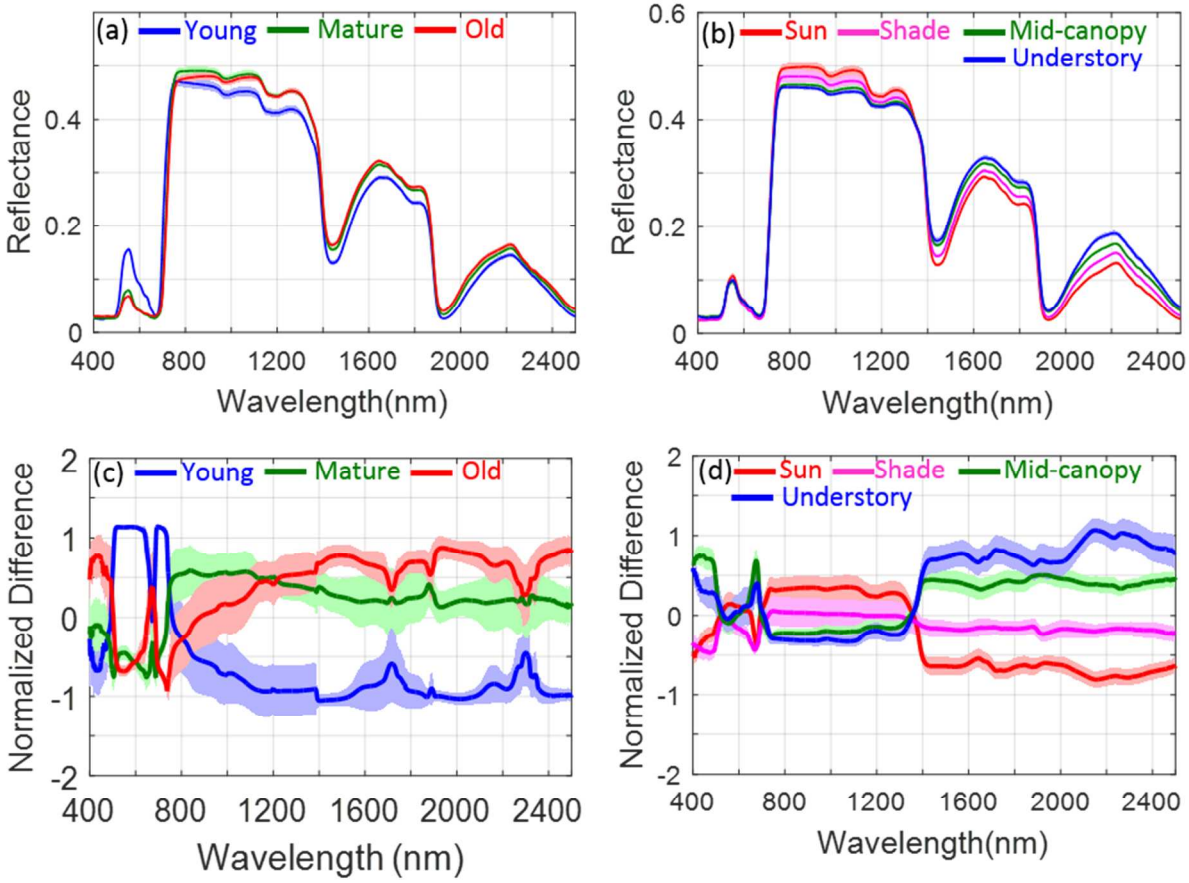

Figure 4. Cross-site spectra-age model results for data from both Peruvian and Brazilian sites, based on fitting variation of the Peru reference Partial Least Squares Regression (PLSR) models to a subset of observations at the Peru site only (i.e., the Peru training dataset): **(a):** Root Mean Square Error (RMSE) between observed and modeled leaf age plotted against the number of latent variables incorporated for PLSR models; **(b):** The proportion of variation in leaf age explained by PLSR models (**R^2**) plotted against the number of latent variables incorporated. Different symbols in (a) and (b) represent different datasets, as indicated (see also Table 1): the performance of the original 7-latent variable model for each dataset is indicated by the points in the blue shaded box in **a, b)**; an optimal model for prediction across sites (RMSE minimized and R^2 maximized for Brazil validation datasets not used in model fitting) emerges for 5 latent variables (gray shaded box in **a, b**). **(c):** Spectral regression coefficients for the optimized PLSR model with 5 latent variables; **(d):** Variable Importance in Projection (VIP) for the optimized PLSR model with 5 latent variables (spectral features greater than 0.8 represent the important spectral regions for leaf age modeling).

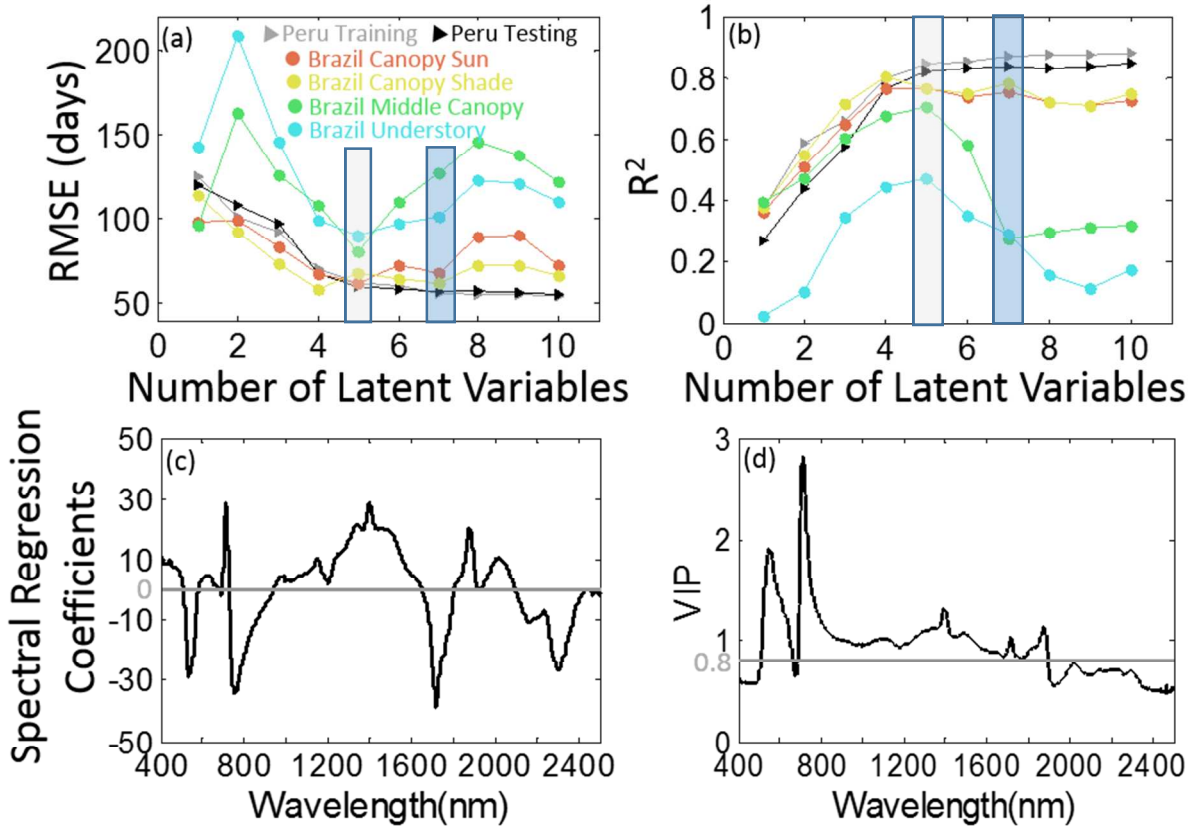

Figure 5. Example of developmental trajectory in a mid-canopy tree in Brazil (*E.uchi*_MC), including: **(a)** the appearance of leaves versus age in RGB photos, showing reddish leaves when leaf ages are 40 days or younger; **(b)** the aging of leaves as revealed by leaf reflectance hyperspectra (measured by an ASD spectradiometer); and **(c)** comparison between spectra-age model coefficients of seven latent variables (in red) and five latent variables (in black), (see Fig. 4; as derived from the model parameterized by Peruvian sunlit canopy leaves, which do not have reddish young leaves). Coefficients in the spectral region marked by the blue window are near-zero in the 5-variable model, which more accurately predicts leaf age in three mid-canopy or understory trees: (d) *E.uchi*_MC, (e) *G. amazonicum*_US, and (f) *M. ruficalyx*_US). The non-zero coefficients in the 7-variable model make it more sensitive to reddish shifts in the understory Brazilian leaves, a confounding effect which causes significant over-prediction of young leaf age in these same trees when the 7-variable model is applied (in g, h, i).

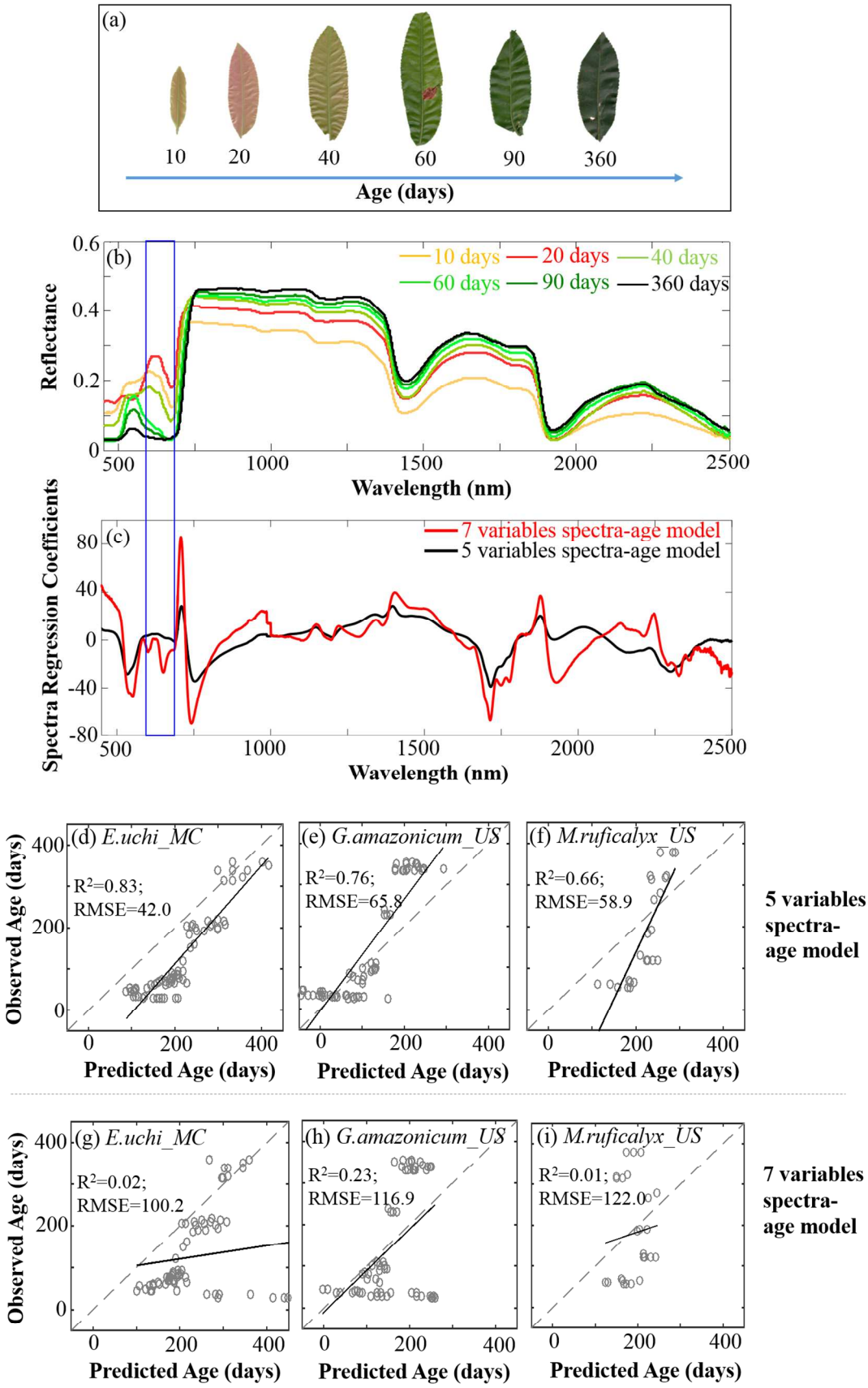
(a)
10
20
40
60
90
360
Age (days)
(b)
10 days
20 days
40 days
60 days
90 days
360 days
Reflectance
Wavelength (nm)
(c)
7 variables spectra-age model
5 variables spectra-age model
Spectra Regression Coefficients
Wavelength (nm)
(d) E.uchi_MC
R²=0.83;
RMSE=42.0
(e) G.amazonicum_US
R²=0.76;
RMSE=65.8
(f) M.ruficalyx_US
R²=0.66;
RMSE=58.9
Observed Age (days)
Predicted Age (days)
5 variables spectra-age model
(g) E.uchi_MC
R²=0.02;
RMSE=100.2
(h) G.amazonicum_US
R²=0.23;
RMSE=116.9
(i) M.ruficalyx_US
R²=0.01;
RMSE=122.0
Observed Age (days)
Predicted Age (days)
7 variables spectra-age model

1097

Figure 6. (a) Branch height probability distribution for Peru (grey line) and Brazil (dark green), with color symbols indicating branch height for each sample; **(b)** Leaf trait scatter plot showing leaf water content (LWC) versus leaf mass per area (LMA) for Peru and Brazil leaf samples from the old leaf age class (Table 1). Red rectangles in (a) and (b) bound the sample space for mid- to upper canopy leaves from Peru and Brazil sites.

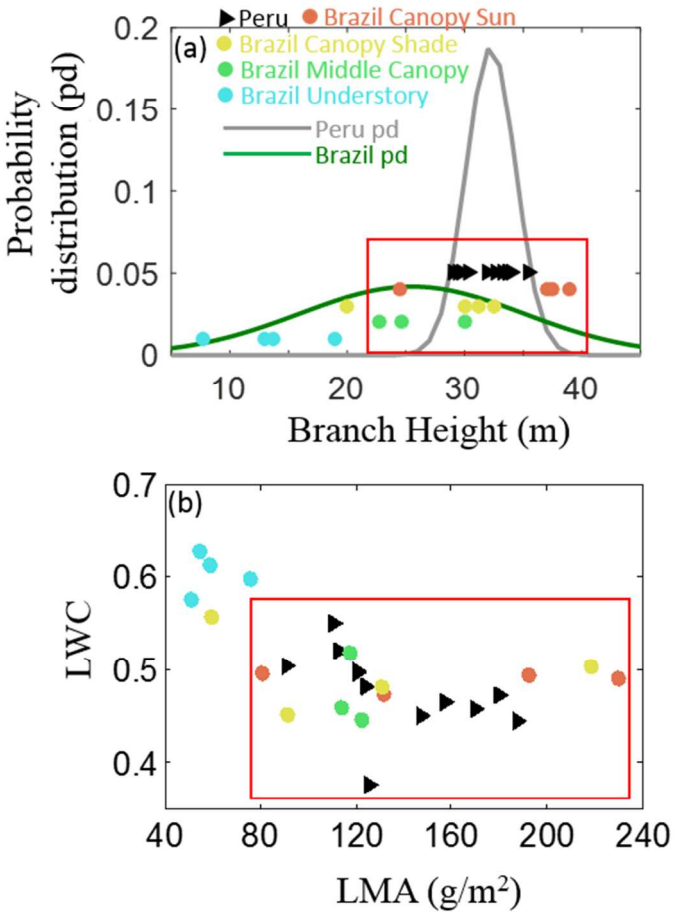

Figure 7. Performance (observed versus predicted leaf age) of the optimal Peru-trained spectral leaf age model (Fig 4, 5-variable model) as applied to Brazilian samples from four canopy environments **(a)-(d):** canopy sun; **(e)-(h)**: canopy shade; **(i)-(k):** mid-canopy; **(l)-(o):** understory. OLS regressions (black lines) quantify the deviation of the scatterplots from the ideal 1:1 line (dashed lines). R^2 quantifies the fit of the regression line – i.e., the variation in leaf age explained by combining the Peru leaf age model (applied to the whole dataset) with the individual tree regressions – and RMSE is the corresponding Root Mean Square Error.

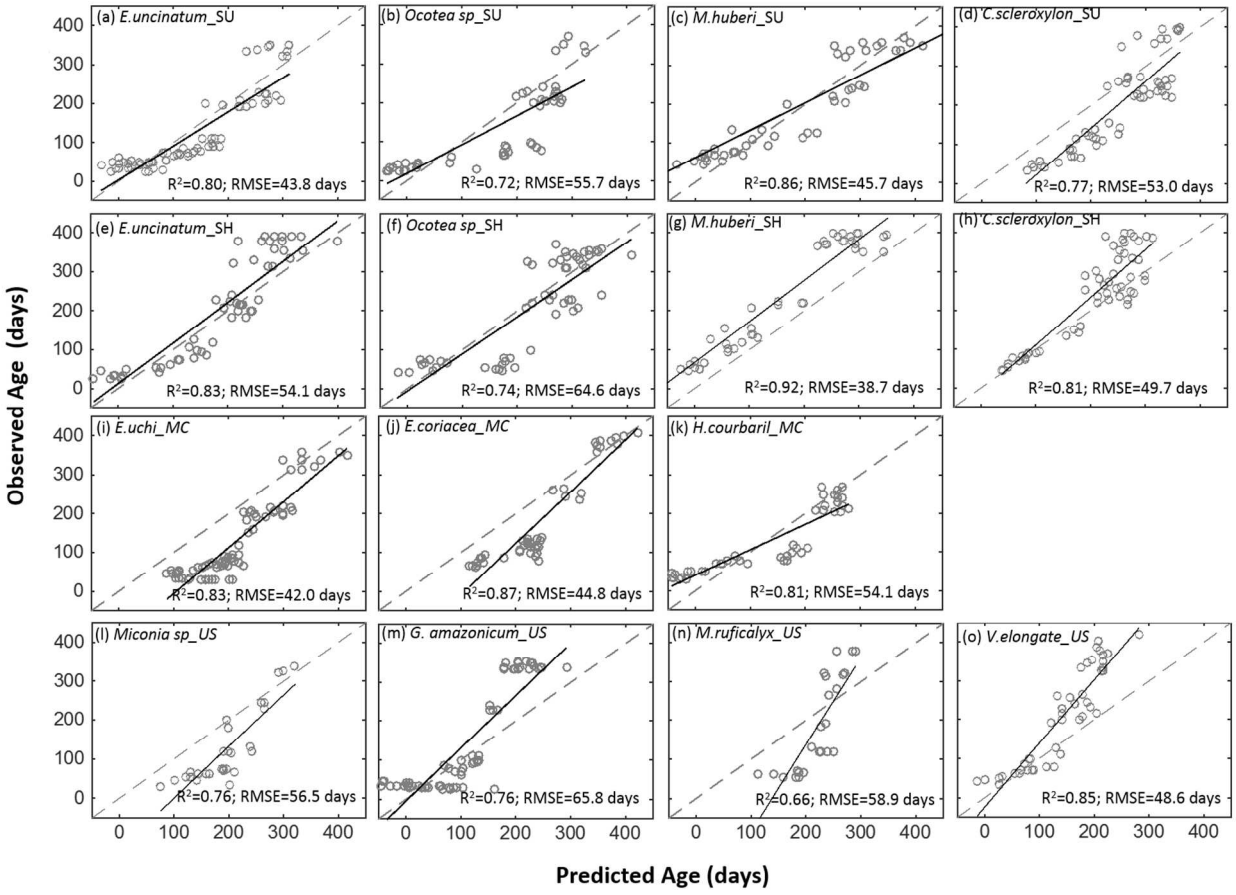

Figure 8. The regression line slopes and intercepts of each tree-environment combination (from Fig. 7) plotted against branch height and leaf mass per area (LMA) for the Brazil site: **(a)** Slope vs. branch height; **(b)** Slope vs. LMA; **(c)** Intercept vs. branch height; **(d)** Intercept vs. LMA.

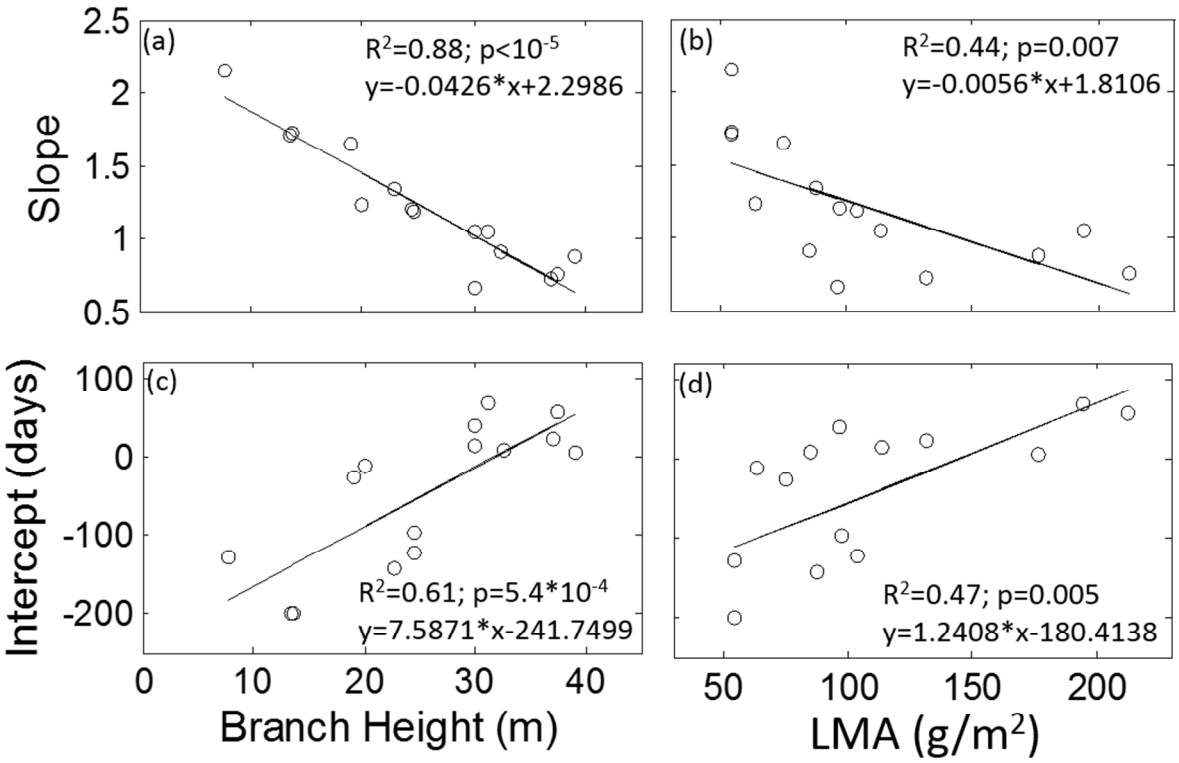

Figure 9. Performance of leaf age models for the Brazilian leaf samples under four scenarios: **(a)** the Peru model (parameterized by using Peruvian leaf spectra only; the same model as presented in Chavana-Bryant *et al.*, 2016 using seven latent variables); **(b)** the Peru reference model optimized for multiple environments (parameterized by using Peruvian leaf spectra only); **(c)** the "Peru Spectra+all Trait" model (parameterized by using Peruvian leaf spectra and traits); **(d)** the "All Spectra" model (parameterized by using both Brazilian and Peruvian leaf spectra); **(e)** the "All Spectra+ all Trait" model (parameterized by using both Brazilian and Peruvian leaf spectra and traits). Four different color circles represent the leaf samples from Brazil canopy sun (red circles; n=4 trees), Brazil canopy shade (yellow circles; n=4), Brazil mid-canopy (green circles; n=3), and Brazil understory trees (blue circles; n=4). Four different color lines represent the corresponding ordinary least regression (OLS) between predicted and observed leaf ages; central grey line represents the OLS analysis for all Brazil samples. The "All Spectra" model (d) is our "recommended" general model. The number of optimal latent variables in panel b was identified in Fig. 4, and in panels c to e were identified in Fig. S6

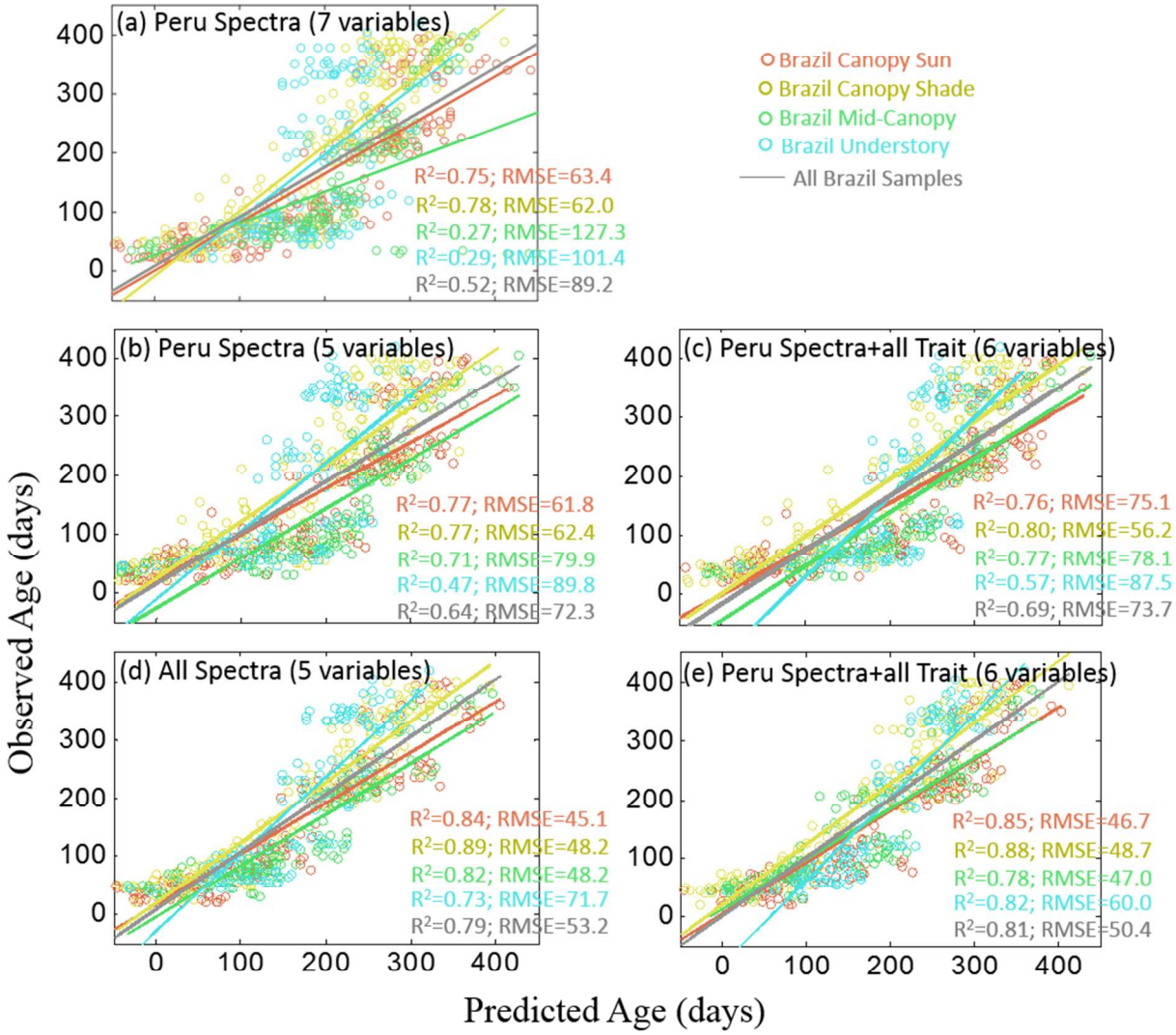
(a) Peru Spectra (7 variables)
R²=0.75; RMSE=63.4
R²=0.78; RMSE=62.0
R²=0.27; RMSE=127.3
R²=0.29; RMSE=101.4
R²=0.52; RMSE=89.2
Brazil Canopy Sun
Brazil Canopy Shade
Brazil Mid-Canopy
Brazil Understory
All Brazil Samples
(b) Peru Spectra (5 variables)
R²=0.77; RMSE=61.8
R²=0.77; RMSE=62.4
R²=0.71; RMSE=79.9
R²=0.47; RMSE=89.8
R²=0.64; RMSE=72.3
(c) Peru Spectra+all Trait (6 variables)
R²=0.76; RMSE=75.1
R²=0.80; RMSE=56.2
R²=0.77; RMSE=78.1
R²=0.57; RMSE=87.5
R²=0.69; RMSE=73.7
(d) All Spectra (5 variables)
R²=0.84; RMSE=45.1
R²=0.89; RMSE=48.2
R²=0.82; RMSE=48.2
R²=0.73; RMSE=71.7
R²=0.79; RMSE=53.2
(e) Peru Spectra+all Trait (6 variables)
R²=0.85; RMSE=46.7
R²=0.88; RMSE=48.7
R²=0.78; RMSE=47.0
R²=0.82; RMSE=60.0
R²=0.81; RMSE=50.4
Observed Age (days)
Predicted Age (days)
0
100
200
300
400

1134

1135

***New Phytologist* Supporting Information**

Article title: Convergence in relations among leaf traits, spectra and age across diverse canopy environments and two contrasting tropical forests

Authors: Jin Wu, Cecilia Chavana-Bryant, Neill Prohaska, Shawn P. Serbin, Kaiyu Guan, Loren P. Albert, Xi Yang, Willem J.D. van Leeuwen, Anthony John Garnello, Giordane Martins, Yadvinder Malhi, France Gerard, Raimundo Cosme Oliviera, and Scott R. Saleska

The following supporting information is available for this article:

Figure S1. Leaf age monitoring at the Brazil site was carried out by using metal tags and *in-situ* photo-documentation. *In-situ* photographs acquired on three different dates illustrate leaf development with age (dates shown are critical time periods for significant changes in leaf size and color as leaf aged) for *M.ruficalyx* (**a-c**; Table 1), for *C.scleroxylon* (**d-f**; Table 1), and for *E.uncinatum.* (**g-i**; Table 1).

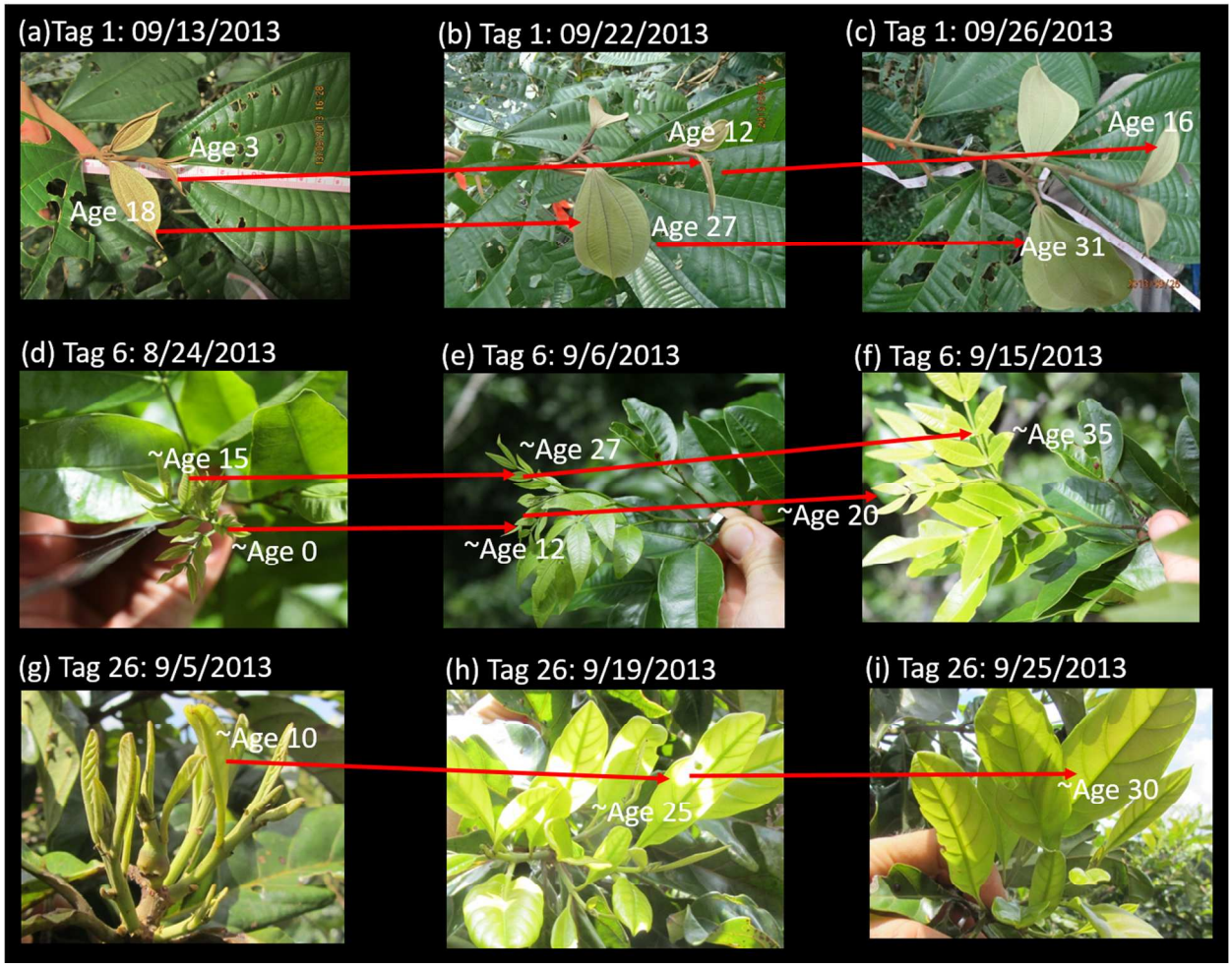

1162 **Figure S2.** Flow-chart for spectra-trait analysis by using Partial Least Squares Regression
1163 (PLSR).

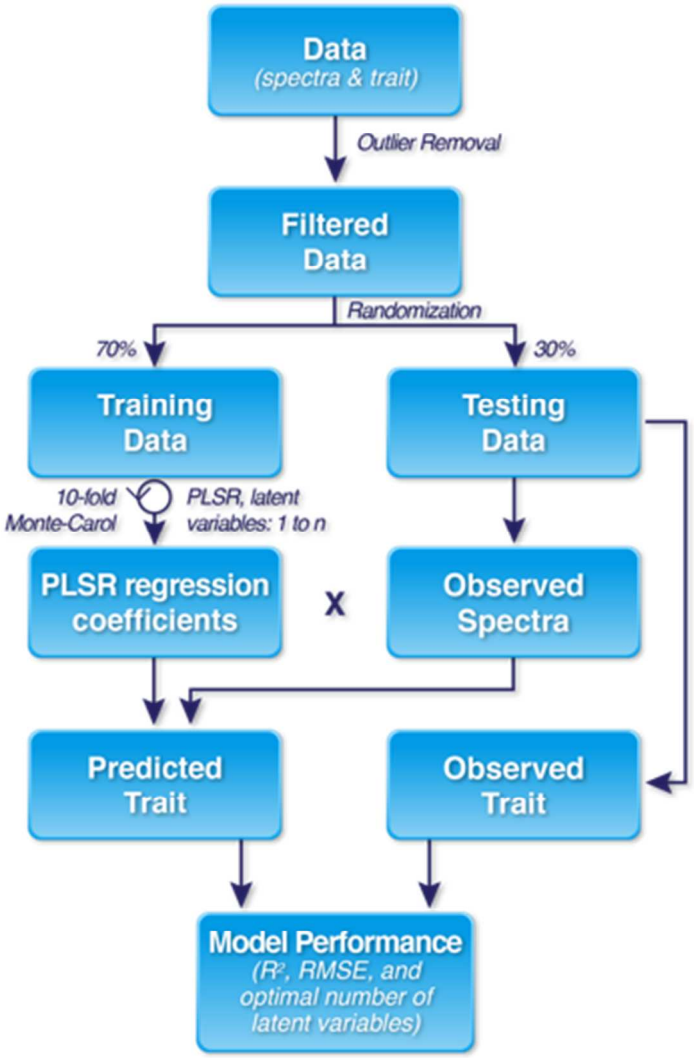

1164
1165
1166
1167

Figure S3. *In situ* Leaf light environments (approximated by gap fraction, derived from hemispherical photos taken above each sampled branch) versus **(a)** branch height above the ground, and **(b)** branch depth below the local canopy top. Each point represents one tree-environment combination. Branch depth is a significantly better proxy of light environment (R^2=0.71) than branch height above the ground is (R^2=0.41).

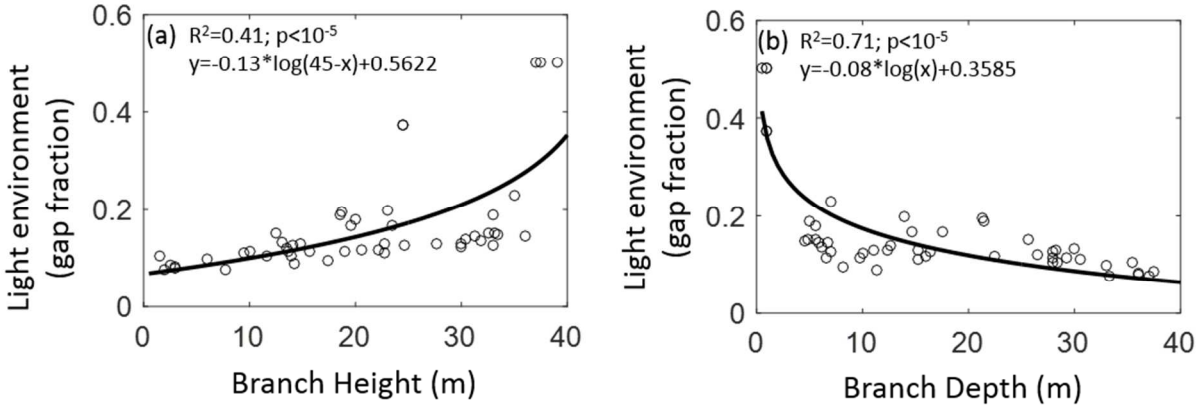

Figure S4. Mature leaf traits versus branch height of sampled leaves above the ground (left column) and branch depth (a strong proxy of light environment, see Fig. S3) of sampled leaves below the local canopy top (right column) at the Brazil site. Traits are: (**a-b**) leaf mass per area (LMA), (**c-d**) leaf water content (LWC), and (**e-f**) leaf level reflectance values (Red at 680 nm and NIR at 800 nm), (**g-h**) leaf level vegetation indices (NDVI (680, 800 nm) and PRI (531, 570 nm)). Samples include all 40 tree species surveyed at the Brazil site (grey circles); the subset of 11 trees whose ages were precisely known and were the basis for the main part of this study (black squares) follow the same pattern as the larger community. Branch height (a proxy integrating effects of both light environment and gravitational component of leaf water potential) is generally a better predictor of leaf traits than branch depth (a proxy of light environment).

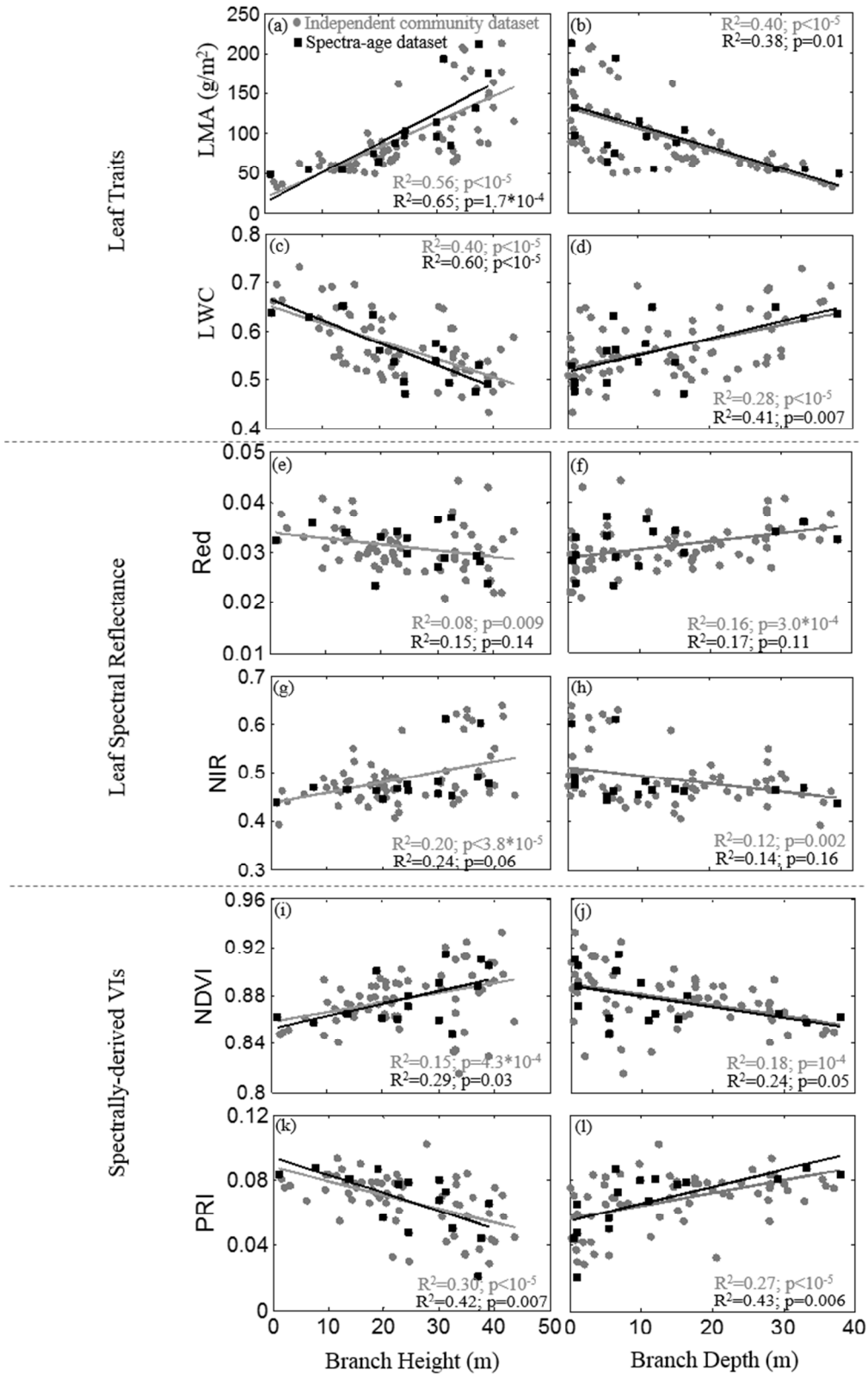
Leaf Traits
Leaf Spectral Reflectance
Spectrally-derived VIs
LMA (g/m²)
LWC
Red
NIR
NDVI
PRI
(a) Independent community dataset
Spectra-age dataset
R²=0.56; p<10⁻⁵
R²=0.65; p=1.7*10⁻⁴
(b)
R²=0.40; p<10⁻⁵
R²=0.38; p=0.01
(c)
R²=0.40; p<10⁻⁵
R²=0.60; p<10⁻⁵
(d)
R²=0.28; p<10⁻⁵
R²=0.41; p=0.007
(e)
R²=0.08; p=0.009
R²=0.15; p=0.14
(f)
R²=0.16; p=3.0*10⁻⁴
R²=0.17; p=0.11
(g)
R²=0.20; p<3.8*10⁻⁵
R²=0.24; p=0.06
(h)
R²=0.12; p=0.002
R²=0.14; p=0.16
(i)
R²=0.15; p=4.3*10⁻⁴
R²=0.29; p=0.03
(j)
R²=0.18; p=10⁻⁴
R²=0.24; p=0.05
(k)
R²=0.30; p<10⁻⁵
R²=0.42; p=0.007
(l)
R²=0.27; p<10⁻⁵
R²=0.43; p=0.006
Branch Height (m)
Branch Depth (m)

1185
1186

1187 **Figure S5.** Leaf age residuals (observed age – modeled age) plotted against observed age, where
1188 the ”All Spectra” model was used here (optimal 5-variable model, Fig. 9d). **(a):** Peru data; **(b):**
1189 Brazil data. The grey circles indicate each individual leaf, and the black lines indicate the
1190 quadratic fitting curve.

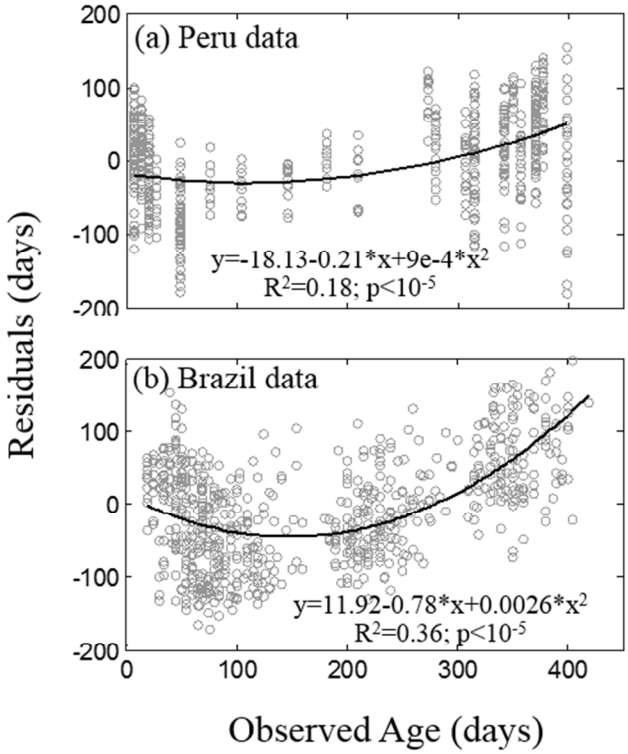

1191
1192
1193

Figure S6. Metrics of fit for PLSR leaf age models versus number of latent variables included in the model for models shown in Fig. 9. **(a)** RMSE and **(b)** R^2 for the "Peru Spectra+all Trait" model; **(c)** RMSE and **(d)** R^2 for the "All Spectra" model; **(e)** RMSE and **(f)** R^2 for the "All Spectra+all Trait" model. Different symbols in (a) and (b) represent different datasets: Peru training data (grey triangles, n=12 trees); Peru testing data (black triangles, n=12); Independent data from the Brazil site, including canopy sun (red circles, n=4), canopy shade (yellow circles, n=4), mid-canopy (green circles, n=3), and understory (blue circles, n=4). Different color lines in (c), (d), (e) and (f) represent different datasets: grey lines—the training data (10 out of 12 trees from Peru, 3 out of 4 trees from Brazilian canopy sun, canopy shade, and understory, respectively, and 2 out of 3 trees from Brazilian mid-canopy); red lines—independent validation data from the remaining data which were not used for model training. The grey shading in all panels indicates the optimum number of latent variables (minimizing RMSE and maximizing R^2 for the independent dataset), including 6 latent variables for the "Peru Spectra+all Trait" model, 5 latent variables for the "All Spectra" model, and 6 latent variables for the "All Spectra+all Trait" model.

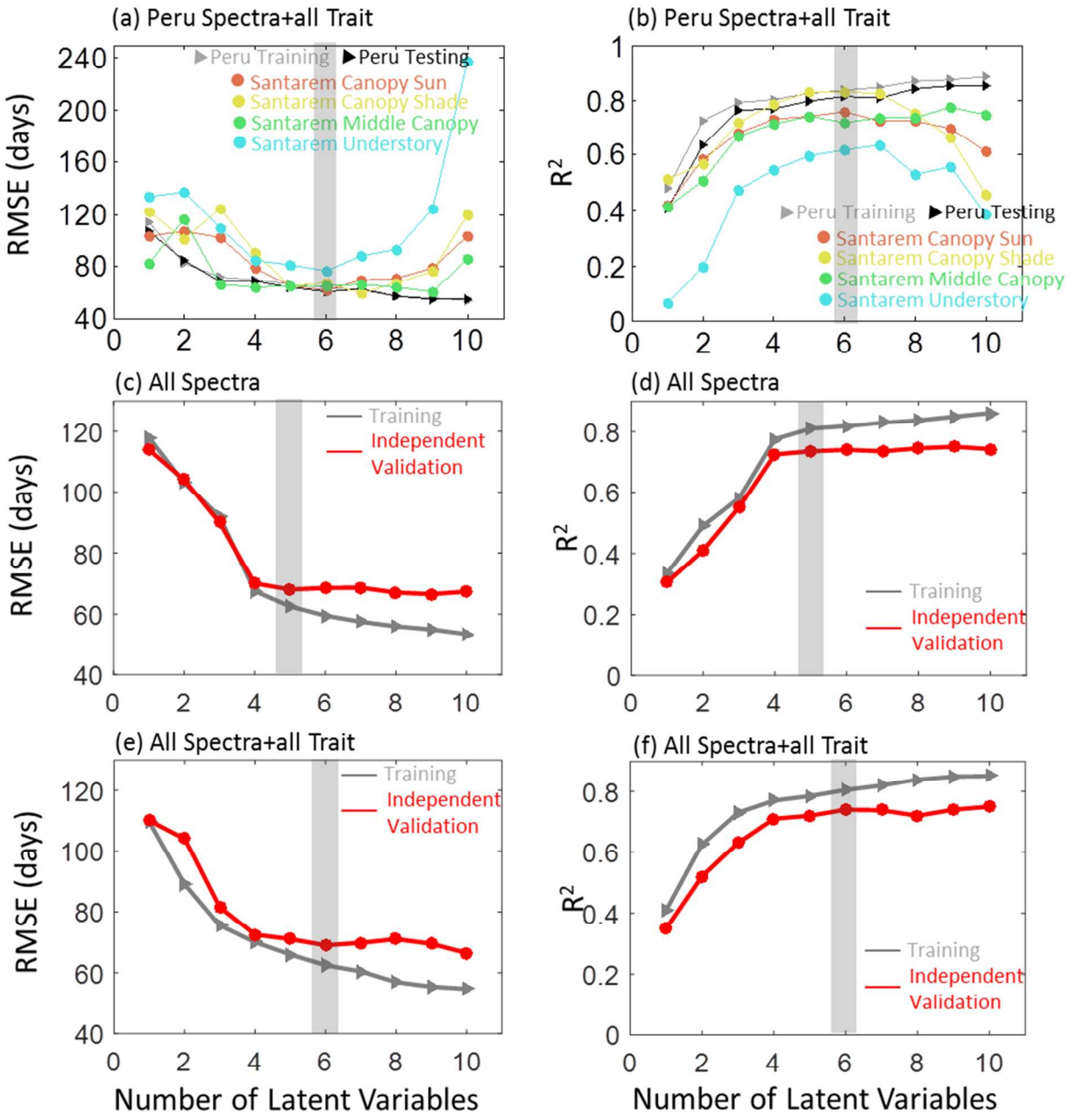
(a) Peru Spectra+all Trait
RMSE (days)
Peru Training
Peru Testing
Santarem Canopy Sun
Santarem Canopy Shade
Santarem Middle Canopy
Santarem Understory
(b) Peru Spectra+all Trait
R2
(c) All Spectra
Training
Independent Validation
(d) All Spectra
(e) All Spectra+all Trait
(f) All Spectra+all Trait
Number of Latent Variables

1210

1211

Figure S7. Mean leaf level hyperspectral reflectance for three leaf age classes at the Brazil site: **(a)** young (20-60 days), **(b)** mature (150-220 days), and **(c)** old (≥300 days) age classes. Different tree-environment combinations are represented by different colored lines and ID codes in the legend (indicated by a *"species name_canopy position"* label in the legend, where "canopy position" is represented by four codes: 'SU' sunlit, 'SH' shaded, 'MC' mid-canopy, and 'US' understory). Solid lines are for canopy leaves, and dashed lines for others.

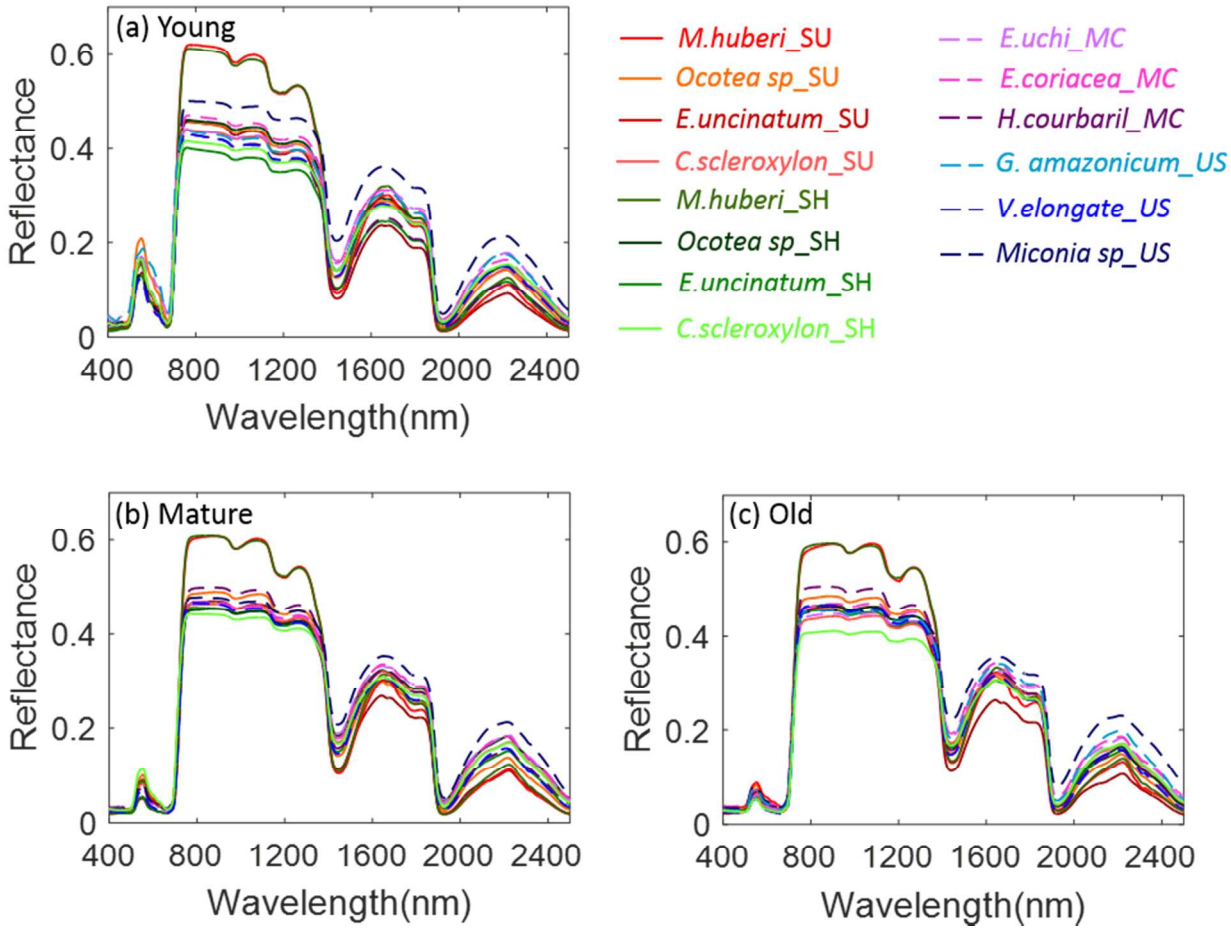

1222 **Table S1.** Summary statistics for leaf traits (LMA gm^{-2} and LWC %) and NIR reflectance (800
1223 nm) under 4 canopy environments and across 2 forest sites. M=mean, SD=standard deviation.
1224 Range=minimum and maximum values, and N=number of leaf samples.

Scenarios	Trait Type		Brazil Canopy Sun	Brazil Canopy Shade	Brazil Mid-Canopy	Brazil Understory	Brazil All	Peru Canopy Sun
Entire leaf life span (7days-400 days)	LMA	M(SD)	149.8 (50.7)	123.0 (58.4)	94.8 (21.4)	58.5 (11.7)	112 (53.6)	116 (37.7)
		Range	69.7-269.5	51.8-245.4	35.3-134.8	40.4-92.0	35.3-269.5	34.6-210.5
		N	150	139	122	93	504	1072
	LWC	M(SD)	52 (5)	55 (5)	53 (8)	66 (4)	56 (8)	56 (10)
		Range	42-68	43-72	42-83	59-79	42-83	34-81
		N	150	139	124	94	507	1072
	NIR	M(SD)	0.51 (0.07)	0.50 (0.08)	0.46 (0.03)	0.47 (0.04)	0.49 (0.06)	0.51 (0.06)
		Range	0.36-0.64	0.38-0.64	0.35-0.52	0.36-0.57	0.35-0.64	0.35-0.69
		N	224	207	186	142	759	1072

1225
1226
1227

Table S2. Leaf age model performance assessment for Brazil data under four scenarios: the "Peru Spectra" model (parameterized by using Peruvian leaf spectra only; five latent variables), the "Peru Spectra+all Trait" model (parameterized by using Peruvian leaf spectra and traits; six latent variables), the "All Spectra" model (parameterized by using both Brazilian and Peruvian leaf spectra; five latent variables), and the "All Spectra+all Trait" model (parameterized by using both Brazilian and Peruvian leaf spectra and traits; six latent variables). Three metrics are used to measure the goodness of model fit, including coefficient of determination (R^2), root-mean-square error (RMSE), and the Akaije Information Criterion (AIC; Akaike, 1974; Aho *et al*., 2014). The AIC was calculated by using the formula $AIC = N \times \log(\delta^2) + 2 \times m$, where N is the number of leaves (summarized in Table S1), δ is RMSE (Fig. 9), and m is the optimum latent variable number used for each PLSR modeling scenario (Fig. S6).

Scenarios	Brazil Canopy Sun			Brazil Canopy Shade			Brazil Mid-Canopy			Brazil Understory			Brazil All		
	R^2	RMSE (days)	AIC	R^2	RMSE (days)	AIC	R^2	RMSE (days)	AIC	R^2	RMSE (days)	AIC	R^2	RMSE (days)	AIC
Peru Spectra	0.77	61.8	1857.5	0.77	62.4	1721.3	0.71	79.9	1639.6	0.47	89.8	1287.3	0.64	72.3	6508.3
All Spectra	0.76	75.1	1948.8	0.80	56.7	1682.0	0.77	78.1	1635.2	0.57	87.5	1283.9	0.69	73.7	6539.4
All Spectra	0.84	45.1	1716.4	0.89	48.2	1614.4	0.82	48.2	1451.6	0.73	71.7	1223.4	0.79	53.2	6042.6
All Spectra +all Trait	0.85	46.7	1736.0	0.88	48.7	1622.7	0.78	47.0	1446.3	0.82	60.0	1176.8	0.81	50.4	5962.5